Mathematical Biosciences and Engineering

http://www.aimspress.com/journal/MBE

MBE, 21(7): 6425–6470.
DOI: 10.3934/mbe.2024281
Received: 28 January 2024
Revised: 04 June 2024
Accepted: 14 June 2024
Published: 01 July 2024

Research article

Mathematical assessment of control strategies against the spread of MERS-CoV in humans and camels in Saudi Arabia

Adel Alatawi [1,2] **and Abba B. Gumel** [3,4,*]

[1] Department of Mathematics, Faculty of Science, University of Tabuk, Tabuk 71491, Saudi Arabia
[2] Biodiversity Genomics Unit, Faculty of Science, University of Tabuk, Tabuk 71491, Saudi Arabia
[3] Department of Mathematics, University of Maryland, College Park, MD, 20742, USA
[4] Department of Mathematics and Applied Mathematics, University of Pretoria, Pretoria 0002, South Africa

* **Correspondence:** Email: agumel@umd.edu.

Abstract: A new mathematical model for the transmission dynamics and control of the Middle Eastern respiratory syndrome (MERS), a respiratory virus caused by MERS-CoV *coronavirus* (and primarily spread to humans by dromedary camels) that first emerged out of the Kingdom of Saudi Arabia (KSA) in 2012, was designed and used to study the transmission dynamics of the disease in a human-camel population within the KSA. Rigorous analysis of the model, which was fitted and cross-validated using the observed MERS-CoV data for the KSA, showed that its disease-free equilibrium was locally asymptotically stable whenever its reproduction number (denoted by $\mathbb{R}_{0M}$) was less than unity. Using the fixed and estimated parameters of the model, the value of $\mathbb{R}_{0M}$ for the KSA was estimated to be 0.84, suggesting that the prospects for MERS-CoV elimination are highly promising. The model was extended to allow for the assessment of public health intervention strategies, notably the potential use of vaccines for both humans and camels and the use of face masks by humans in public or when in close proximity with camels. Simulations of the extended model showed that the use of the face mask by humans who come in close proximity with camels, as a sole public health intervention strategy, significantly reduced human-to-camel and camel-to-human transmission of the disease, and this reduction depends on the efficacy and coverage of the mask type used in the community. For instance, if surgical masks are prioritized, the disease can be eliminated in both the human and camel population if at least 45% of individuals who have close contact with camels wear them consistently. The simulations further showed that while vaccinating humans as a sole intervention strategy only had marginal impact in reducing the disease burden in the human population, an intervention strategy based on vaccinating camels only resulted in a significant reduction in the disease burden in camels (and, consequently, in humans as well). Thus, this study suggests that attention should be focused on effectively combating the disease in the camel population, rather than in the human population. Furthermore, the extended

model was used to simulate a hybrid strategy, which combined vaccination of both humans and camels as well as the use of face masks by humans. This simulation showed a marked reduction of the disease burden in both humans and camels, with an increasing effectiveness level of this intervention, in comparison to the baseline scenario or any of the aforementioned sole vaccination scenarios. In summary, this study showed that the prospect of the elimination of MERS-CoV-2 in the Kingdom of Saudi Arabia is promising using pharmaceutical (vaccination) and nonpharmaceutical (mask) intervention strategies, implemented in isolation or (preferably) in combination, that are focused on reducing the disease burden in the camel population.

Keywords: MERS-CoV-2; dromedary camels; vaccination; face mask; reproduction number

1. Introduction

Middle Eastern respiratory syndrome (MERS), a respiratory virus caused by MERS-CoV *coronavirus*, first emerged in Jeddah, Saudi Arabia, on June 13, 2012 [1–4]. The disease, which is of the same genealogy as SARS-CoV-1 (which emerged in 2002–2003) and SARS-CoV-2 (which emerged in 2019) (see Table 1 for a comparison of the three human coronaviruses), rapidly spread to numerous countries (including Algeria, Austria, Bahrain, China, Egypt, France, Germany, Greece, Iran, Italy, Jordan, Kuwait, Lebanon, Malaysia, Netherlands, Oman, Philippines, Qatar, Republic of Korea, Thailand, Tunisia, Turkey, United Kingdom, United Arab Emirates, United States, and Yemen) [2, 5]. Data from the World Health Organization report for May 2023 showed that MERS caused 2604 confirmed cases and 936 deaths (representing a 36% case-fatality ratio) globally (as of June 5, 2023). Furthermore, the Kingdom of Saudi Arabia (KSA) and the Republic of Korea recorded the majority of the global MERS-CoV cases (in particular, the KSA reported 2196 cases and 855 deaths) [6, 7] (Figure 1 depicts the number of weekly new cases of MERS-CoV for the KSA). The KSA is vulnerable to MERS-CoV-2 outbreaks due to the numerous large gathering events it hosts, notably the annual Hajj pilgrimage (once a year) and Umrah year [8], and the camel festival in Riyadh (which runs for a two-month period) [9, 10].

Several empirical studies have shown that bats and dromedary camels are the main reservoir hosts of MERS-CoV [11–15] (see Figure 2). Transmission from camel to camel or camel to human could occur by contact with the animal's nasal secretions, saliva, or respiratory droplets [16, 17]. MERS-CoV spreads among dromedary camels *via* respiratory routes [18], and dromedary camels infected with MERS-CoV exhibit symptoms (typically manifesting within two days and continue for up to two weeks [19]) which include mucopurulent nasal and lachrymal discharge, appetite loss, fever, rhinorrhea (runny nose), coughing, and sneezing [19]. The disease is primarily transmitted to humans by infected dromedary camels [2, 11, 17, 20–22] through inhalation of respiratory droplets and airborne particles. The virus could also be transmitted to humans after drinking the raw milk or eating the meat of infected camels [17, 19, 23]. Other potential sources of MERS-CoV transmission from camels to humans include crowding (i.e., camel-to-camel or camel-to-human), mixing camels from different regions, transportation of camels, and markets for trade of live animals [17, 21, 24]. Furthermore, camel racing and camel show festivals (where camels are kept in a large space for 2 months [18]) increases the likelihood of MERS-CoV transmission between camels and humans [18, 19, 25] (MERS-CoV can

be detected in viral RNA in camels for up to 35 days post-inoculation [26, 27]). Furthermore, although the mechanisms for camel-to-human transmission of MERS-CoV are well-understood, there is a general lack of knowledge of the mechanism resulting in human-to-camel transmission of MERS-CoV [17, 18, 28, 29]. MERS-CoV transmission from human to human is well-documented in family clusters, community settings, and more frequently in healthcare settings [19, 30–33]. Finally, MERS-CoV can also be transmitted through direct contact with contaminated objects and surfaces [34–37].

Table 1. Comparison of epidemiological and clinical characteristics of novel coronaviruses [34, 38, 39].

Characteristics	SARS-CoV-1	MERS-CoV	SARS-CoV-2
Origin location	Guandong, China	Jeddah, Saudi Arabia	Wuhan, China
Duration	2002–2003	2012–to date	Dec. 2019–to date
Reservoir	Bats & civet cats	Bats & camels	Bats (Pangolins)
Countries	29	27	220
Incubation period	2–7 days	5 days	2–14 days
Confirmed cases	8098	2604	676,609,955
Global deaths	774	936	6,881,955
Cases-fatality ratio	9.5%	36%	1%

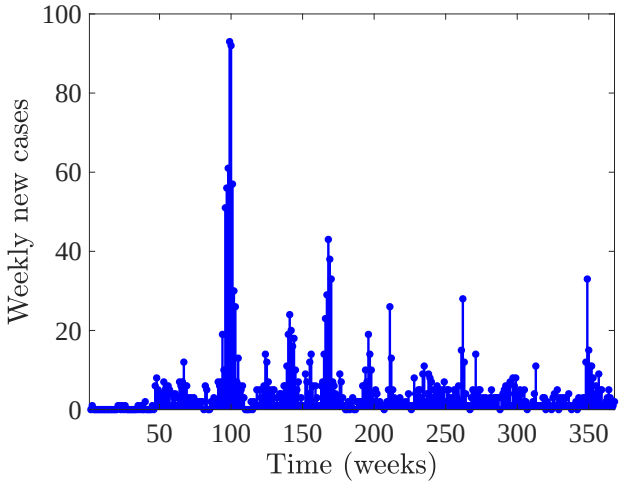

Figure 1. Weekly new cases of MERS-CoV in the Kingdom of Saudi Arabia for the period from the second week of June 2012 to the fourth week of June 2019 [6].

The main non-pharmaceutical interventions (NPIs) implemented against MERS-CoV in the KSA were focused on preventing human-to-human transmission (notably reducing the likelihood of inhaling infected respiratory droplets and minimizing contacts with infected humans [40]) and minimizing or avoiding contacts with infected camels [29, 41]. Consequently, the main NPIs implemented against MERS-CoV in the KSA include the use of face masks by humans who are within close proximity (typically a meter) of MERS-infected individuals and avoiding contact with MERS-infected patients during visitations in a healthcare setting [40]. Furthermore, individuals who have close contact with

camels are encouraged to wear proper personal protective equipment (PPE), especially N95 masks, surgical gowns, and goggles [18, 42].

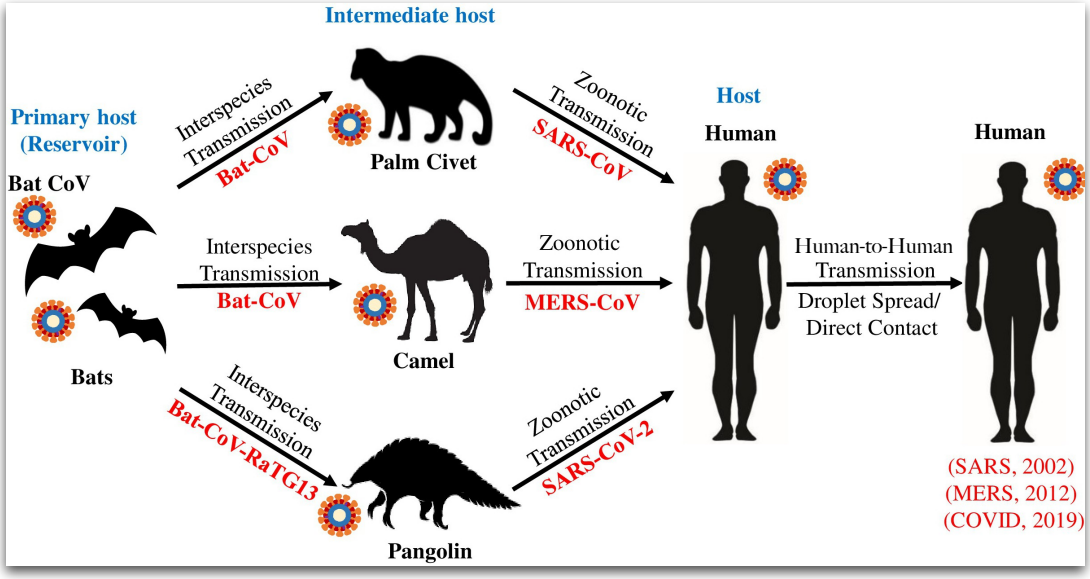

Figure 2. Zoonotic origins and transmission pathways of novel human coronaviruses [43].

To reduce the likelihood of MERS-CoV transmission through the consumption of infected milk, the Saudi Ministry of Health strongly recommended that camel milk should be thoroughly boiled or pasteurized before use. Similarly, it is strongly advised that camel meat must be thoroughly cooked before consumption [18, 42]. Healthcare workers are at a high risk of acquiring a MERS-CoV infection (they account for 31% of transmission [44, 45]). Thus, healthcare workers are strongly encouraged to wear N95 respirators (data showed a marked reduction, by at least 56%, in sero-positivity, in comparison to healthcare workers who do not, or rarely, wear N95 masks [42]). The importation and transportation of dromedary camels between nations is another major risk factor for MERS-CoV transmission [19, 42]. Camels destined for exportation are tested in the originating country for the presence of MERS-CoV antibodies and antigens [19,42]. Upon arrival at the destination country, the camels are typically placed in quarantine while being sampled and tested for MERS-CoV. Before being allowed to be imported into the country, camels that have tested positive for MERS-CoV or are sero-positive are isolated at border crossings. Camels brought for other objectives, such as breeding and racing competitions, also represent a high risk of MERS-CoV transmission to the indigenous camel breeds (because they will eventually be mixed with the indigenous herds). Camels suspected of being infected with MERS-CoV are transported internally in properly equipped, closed, and ventilated vehicles. Furthermore, in general, camels are not crammed too closely together in a single vehicle [42].

Although there is currently no authorized antiviral medication or vaccine to protect humans from MERS-CoV [2, 27, 46–51], there, however, are two candidate anti-MERS human vaccines (produced by Novavax and Greffex Inc.) currently undergoing advanced stages of clinical trials [2, 48, 52]. Additionally, some potentially promising vaccines are being developed for use in camels [53]. For example, the biotechnology company INOVIO, in collaboration with the Coalition for Epidemic Preparedness Innovations (CEPI), developed a DNA-based human MERS-CoV vaccine that is currently

at the second stage of clinical trials [54]. Furthermore, INOVIO, in collaboration with GeneOne Life Science Inc., developed a DNA-based vaccine [53] that is also undergoing the second stage of clinical trials in humans [51, 55]. Finally, Johnson & Johnson, in collaboration with CEPI and the Jenner Institute at the University of Oxford, is currently designing an adenovirus-based vaccine against MERS-CoV in humans [56]. Similarly, although there are currently no vaccines against MERS-CoV in camels [2,27,46–51], some promising candidate vaccines are undergoing clinical trials. These include: recombinant DNA and protein-based vaccines, subunit vaccines, viral vector-based vaccines (including vaccines designed based on using the measles viral vector, Poxviral vector, human adenoviral vectors, and Chimpanzee adenoviral vectors) [53]. INOVIO, in collaboration with GeneOne Life Science Inc., developed a DNA-based vaccine [53] that was tested in dromedary camels, showing encouraging protective outcomes against the disease [51, 53]. An adenovirus-based vaccine developed by researchers from the University of Oxford is being tested in dromedary camels and humans [47, 51, 53, 57].

Mathematical models of varying types (such as compartmental [2, 28, 58, 59], statistical [60, 61], and stochastic [15,62–64]) have been developed and used to study the transmission dynamics and control of MERS-CoV in camel, human, or human and camel populations. For example, compartmental models were formulated and used to study the transmission dynamics of MERS-CoV among humans, camels, and between humans and camels [2, 28, 31, 59, 65, 66]. One of the earliest MERS-CoV models was a two-group compartmental model developed by Malik [2] to study the dynamics of the disease in a mass gathering of humans (specifically, during the Hajj and Umrah gatherings in the Kingdom of Saudi Arabia [2]). The study proposed optimal strategies, based on the quarantine of suspected cases, the isolation of symptomatic individuals, and the use of a potential future vaccine, for effectively combating or mitigating the disease during those mass gathering events. Ghosh and Nadim [28] used a compartmental model of two co-circulating zoonotic MERS-CoV strains to study the spread of the disease in both humans and camels. This study emphasized preventive measures for susceptible humans and the isolation of infected camels. Chowell et al. [15] evaluated the multiple MERS-CoV transmission routes in humans using a stochastic model. The study, which used epidemiological data for the MERS-CoV outbreak that occurred in the KSA during April to October of 2013 [15], discussed the uncertainty in epidemic risk while taking observation bias in their consideration. They match the evaluation of MERS-CoV cases during that period with a dynamic transmission model that included community and hospital compartments.

Since the KSA attracts such mass gatherings from around the world every year (and year-around), the main motivation of the current study is that effectively controlling outbreaks of MERS-CoV in the KSA could prevent the likelihood of a major global pandemic starting from the KSA. The objective of this study is to use mathematical modeling approaches, together with data analytics and computation, to study the transmission dynamics of the MERS-CoV endemic in the KSA. Specifically, the objective will be achieved by, first, using a basic deterministic model that captures the essential epidemiological and biological features of the disease. The basic model, which will be parameterized using observed cumulative MERS-CoV case data for the KSA, will be rigorously analyzed to gain insight into its qualitative features (with respect to the existence and asymptotic stability of its associated equilibria). Numerical simulations will be carried out to assess the population-level impacts of various control and mitigation strategies. The basic model will then be extended to allow for the assessment of the population-level impact of public health intervention (pharmaceutical and non-pharmaceutical), notably face mask usage and the vaccination of both humans and camels. The extended model will also

be rigorously analyzed and simulated.

The paper is organized as follows. The basic model (2.1) is formulated, and its basic qualitative properties analyzed, in Section 2.1. The basic model is also fitted with the cumulative cases data for the Kingdom of Saudi Arabia in Section 3.2. The basic model is rigorously analyzed, with respect to the existence and asymptotic stability of its associated equilibria, in Section 3. Furthermore, the basic model is extended in Section 4.1 to incorporate the aforementioned intervention and control strategies. The extended model is rigorously analyzed and simulated in Sections 4.2 and 5, respectively.

2. Materials and methods

2.1. Formulation of the basic model

To develop the basic mathematical model for the transmission dynamics of MERS-CoV within and across human and dromedary camel populations in the KSA, the total human population in the KSA at time t, denoted by $N_H(t)$, is split into the mutually exclusive compartments of susceptible ($S_H(t)$), exposed ($E_H(t)$), asymptomatically infectious ($I_{HA}(t)$), symptomatically infectious ($I_{HS}(t)$), hospitalized ($I_{HH}(t)$), and recovered ($R_H(t)$) humans, so that:

$$N_H(t) = S_H(t) + E_H(t) + I_{HA}(t) + I_{HS}(t) + I_{HH}(t) + R_H(t).$$

Similarly, the total population of dromedary camels in the KSA at time t, denoted by $N_C(t)$, is subdivided into the sub-populations of susceptible ($S_C(t)$), exposed ($E_C(t)$), infectious ($I_C(t)$), and recovered ($R_C(t)$) camels. Hence,

$$N_C(t) = S_C(t) + E_C(t) + I_C(t) + R_C(t).$$

The equations for the dynamics of MERS-CoV in a humans-camels community is given by the following deterministic system of nonlinear differential equations [4]:

$$\begin{aligned}
\dot{S}_H &= \Pi_H - \lambda_H S_H - \lambda_{CH} S_H - \mu_H S_H,\\
\dot{E}_H &= \lambda_H S_H + \lambda_{CH} S_H - (\sigma_H + \mu_H) E_H,\\
\dot{I}_{HA} &= r\sigma_H E_H - (\gamma_{HA} + \mu_H + \delta_{HA}) I_{HA},\\
\dot{I}_{HS} &= (1-r)\sigma_H E_H - (\phi_{HS} + \gamma_{HS} + \mu_H + \delta_{HS}) I_{HS},\\
\dot{I}_{HH} &= \phi_{HS} I_{HS} - (\gamma_{HH} + \mu_H + \delta_{HH}) I_{HH},\\
\dot{R}_H &= \gamma_{HA} I_{HA} + \gamma_{HS} I_{HS} + \gamma_{HH} I_{HH} - \mu_H R_H,\\
\dot{S}_C &= \Pi_C + \psi_C R_C - \lambda_C S_C - (\lambda_{HC_A} + \lambda_{HC_S}) S_C - \mu_C S_C,\\
\dot{E}_C &= \lambda_C S_C + (\lambda_{HC_A} + \lambda_{HC_S}) S_C - (\sigma_C + \mu_C) E_C,\\
\dot{I}_C &= \sigma_C E_C - (\gamma_C + \mu_C + \delta_C) I_C,\\
\dot{R}_C &= \gamma_C I_C - (\psi_C + \mu_C) R_C,
\end{aligned} \tag{2.1}$$

where the infection rates for MERS CoV-2 transmission from human to human (λ_H), camel to camel (λ_C), camel to human (λ_{CH}), asymptomatically infectious human to camel (λ_{HC_A}), and symptomatically infectious humans to camel (λ_{HC_S}) are given, respectively, by:

$$\lambda_H = \frac{\beta_{HH}\left[\eta_{HA}I_{HA} + I_{HS} + \eta_{HH}I_{HH}\right]}{N_H},\ \lambda_C = \frac{\beta_{CC}I_C}{N_C},\ \lambda_{CH} = \frac{\beta_{CH}I_C}{N_C},$$
$$\lambda_{HC_A} = \frac{\beta_{HC}\,\eta_{HA}I_{HA}}{N_H},\quad \lambda_{HC_S} = \frac{\beta_{HC}I_{HS}}{N_H}. \tag{2.2}$$

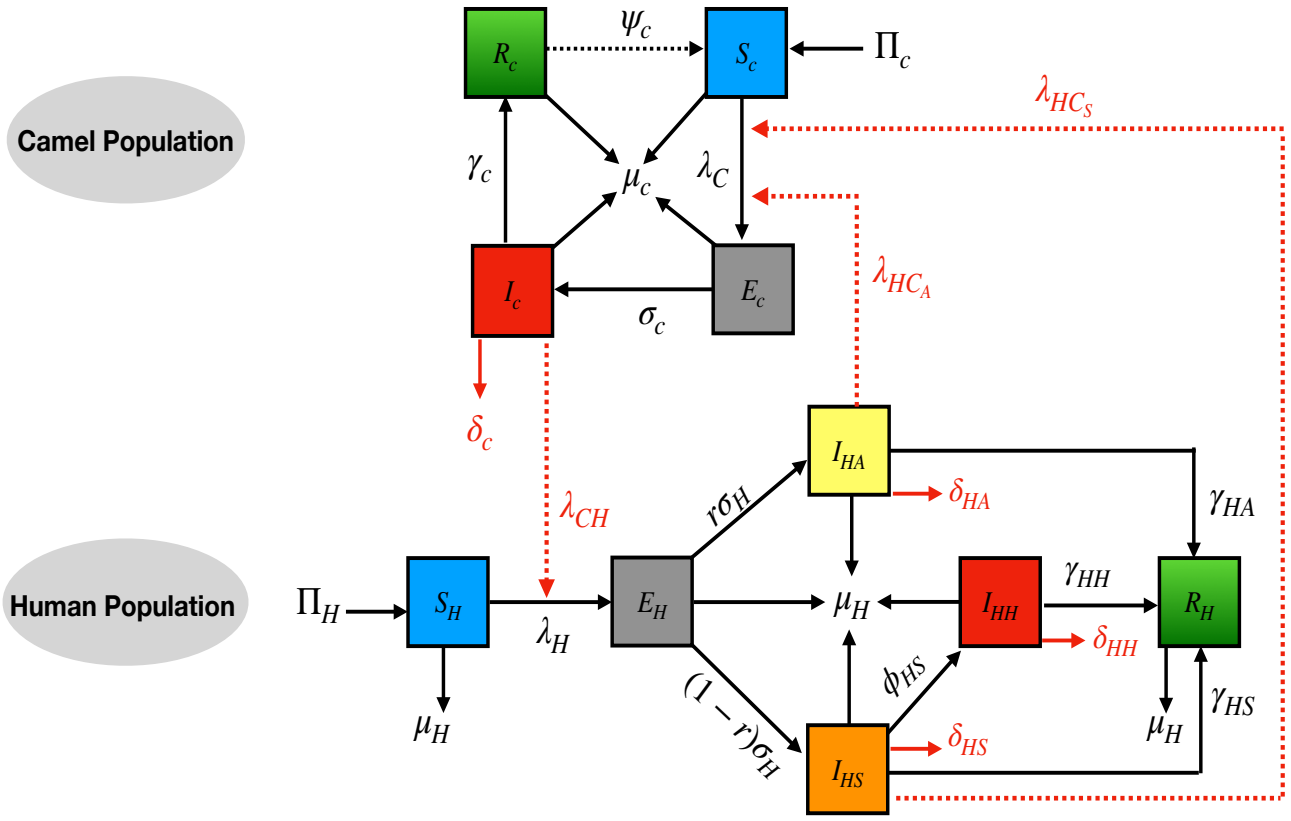

Figure 3. Flow diagram of the model (2.1), where the infection rates λ_H, λ_C, λ_{CH}, λ_{HC_A}, and λ_{HC_S} are as given in (2.2) [4].

In the model (2.1), Π_H (Π_C) is the recruitment of humans (camels) into the population (all newly recruited humans and camels are assumed to be susceptible to MERS-CoV), and β_{HH} (β_{CC}) represents the rate at which MERS-CoV is transmitted to susceptible humans (camels). β_{HC} (β_{CH}) represents the rate at which MERS-CoV is transmitted from humans to camels (camels to humans). The parameter μ_H (μ_C) represents the natural death rate of humans (camels). We differentiate the transmission probability of symptomatic and hospitalized individual with the respective weights, $0 < \eta_{HA}, \eta_{HH} < 1$. Exposed

humans (camels) become infectious at a rate of σ_H (σ_C) (i.e., $1/\sigma_H$ ($1/\sigma_C$) is the average duration from the initial infection to infectiousness for humans (camels)). The proportion r of these humans who become infectious after surviving the exposed class show no clinical symptoms of MERS-CoV, and move to the asymptomatically infectious class I_{HA} (at a rate $r\,\sigma_H$), and the remaining proportion, $1-r$, show clinical symptoms of MERS-CoV and move to the symptomatic class I_{HS} (at a rate $(1-r)\sigma_H$). The parameter $\gamma_{HA}(\gamma_{HS})(\gamma_{HH})(\gamma_C)$ represents the rate at which asymptomatic (symptomatic)(hospitalized) humans (camels) recover from MERS-CoV infection. The parameter $\delta_{HA}(\delta_{HS})(\delta_{HH})(\delta_C)$ is the disease induced mortality rate for asymptomatic (symptomatic) (hospitalized) humans (camels). Let $D_H(t)$ and $D_C(t)$ represent the total number of humans and camels, respectively, who died of MERS-CoV at time t. Hence, the rates of change of the deceased human and camel populations are given, respectively, by:

$$\dot{D_H} = \delta_{HA} I_{HA} + \delta_{HS} I_{HS} + \delta_{HH} I_{HH}, \tag{2.3}$$

and

$$\dot{D_C} = \delta_C I_C. \tag{2.4}$$

A flow diagram of the model (2.1) is depicted in Figure 3, and the state variables and parameters of the model are described in Tables 5 and 6, respectively [4].

The main assumptions made in the formulation of the model (2.1) are:

1) Exponentially distributed waiting times in each epidemiological compartment for humans and camels [15, 67].

2) Well-mixed homogeneous human and camel populations: it is assumed that the populations for humans and camels are well-mixed, and that every member of the community (human or camel) has equal likelihood of mixing with every other member of the community. Furthermore, every member has equal probability of acquiring and/or transmitting infection to hosts of the same or different types (i.e., human to camel and camel to human) [2, 15].

3) It is assumed that between-species transmission occurs at a reduced rate, in comparison to within-species transmission (i.e., humans (camels) are assumed to transmit to camels (humans) at a lower rate, in comparison to human-to-human (camel-to-camel) transmission [28, 66].

4) Hospitalized humans do not transmit infection to camels.

5) Humans who have recovered from MERS-CoV acquire lasting (and permanent) natural immunity against re-infection [2, 28]. However, recovered camels can lose their infection-acquired immunity and become susceptible again [63].

6) Since MERS-CoV has been in circulation for more than ten years in the Kingdom of Saudi Arabia, it is assumed to be *endemic* (so that the demographic (birth and natural death parameters) processes are accounted for in the model).

The basic qualitative properties of the model (2.1) will now be assessed.

2.2. Basic qualitative properties of the model (2.1)

Since the model (2.1) monitors the temporal dynamics of the populations of humans and camels, all its associated parameters and state variables are non-negative for all $t \geq 0$. We claim the following non-negativity result for the model:

Theorem 2.1. *Consider the closed sets*

$$\mathbb{D}_H = \left\{(S_H, E_H, I_{HA}, I_{HS}, I_{HH}, R_H) \in \mathbb{R}_+^6\right\} \text{ and } \mathbb{D}_C = \left\{(S_C, E_C, I_C, R_C) \in \mathbb{R}_+^4\right\}.$$

The region

$$\mathbb{D} = \mathbb{D}_H \cup \mathbb{D}_C$$

is positively invariant and attracting with respect to the model (2.1).

Proof. Adding the first six and the last four equations of the model (2.1) gives, respectively,

$$\begin{aligned} \dot{N}_H &= \Pi_H - \mu_H N_H - (\delta_{HA} I_{HA} + \delta_{HS} I_{HS} + \delta_{HH} I_{HH}), \\ \dot{N}_C &= \Pi_C - \mu_C N_C - \delta_C I_C. \end{aligned} \tag{2.5}$$

Since all of the parameters of the model (2.1) are non-negative, it follows from (2.5) that

$$\dot{N}_H(t) \leq \Pi_H - \mu_H N_H(t), \tag{2.6}$$

and

$$\dot{N}_C(t) \leq \Pi_C - \mu_C N_C(t). \tag{2.7}$$

$N_C(t) \geq \Pi_C/\mu_C$, respectively. Consequently, it follows from (2.6), using the comparison theorem [68], that:

$$N_H(t) \leq N_H(0)e^{-\mu_H(t)} + \Pi_H/\mu_H[1 - e^{-\mu_H(t)}].$$

Similarly, it follows from (2.7) that:

$$N_C(t) \leq N_C(0)e^{-\mu_C(t)} + \Pi_C/\mu_C[1 - e^{-\mu_C(t)}].$$

In particular, $N_H(t) \leq \Pi_H/\mu_H$ if $N_H(0) \leq \Pi_H/\mu_H$ and $N_C(t) \leq \Pi_C/\mu_C$ if $N_C(0) \leq \Pi_C/\mu_C$, respectively. Thus, if $N_H(0) > \Pi_H/\mu_H$, then either the solution of the human component of the model enters $\mathbb{D}_H$ in finite time, or $N_H(t)$ approaches Π_H/μ_H and the infected variables $E_H(t), I_{HA}(t), I_{HS}(t)$, and $I_{HH}(t)$ approach zero as $t \to \infty$ [69]. Hence, the feasible region $\mathbb{D}_H$ is invariant and attracting (i.e., all solutions of the human component of the model lie in, or eventually enter, $\mathbb{R}_+^6$). Similarly, it can be seen that if $N_C(0) > \Pi_C/\mu_C$, then either the solution of the camel component of the model enters $\mathbb{D}_C$ in finite time, or $N_C(t)$ approaches Π_C/μ_C (and the infected variables $E_C(t)$ and $I_C(t)$ approach zero as $t \to \infty$ [69]). Hence, $\mathbb{D}_C$ is also positively invariant and attracting. Since the union and intersection of invariant sets is also invariant [70, 71], it follows that $\mathbb{D}$ is positively invariant and attracting with respect to the model.

The epidemiological consequence of Theorem 2.1 is that the model (2.1) is well-posed and mathematically and epidemiologically in the region $\mathbb{D}$ (hence, it is sufficient to consider the dynamics of the flow generated by the model (2.1) in $\mathbb{D}$ [72]).

3. Theoretical analysis

3.1. Existence and asymptotic stability of disease-free equilibrium

The model (2.1) has a unique disease-free equilibrium (DFE) given by:

$$\mathbb{E}_0 = (S_H^*, E_H^*, I_{HA}^*, I_{HS}^*, I_{HH}^*, R_H^*, S_C^*, E_C^*, I_C^*, R_C^*) = (\Pi_H/\mu_H, 0, 0, 0, 0, 0, \Pi_C/\mu_C, 0, 0, 0)\,. \tag{3.1}$$

It follows, using the next-generation operator method [73, 74], that the DFE of the model is locally asymptotically stable if the spectral radius of the matrix FV^{-1} is less than one, where matrices F (of the new infection terms) and V (of the linear transition terms in the infected compartments) are given, respectively, by:

$$F = \begin{bmatrix} 0 & \beta_{HH}\eta_{HA}\left(\frac{S_H^*}{N_H^*}\right) & \beta_{HH}\left(\frac{S_H^*}{N_H^*}\right) & \beta_{HH}\eta_{HH}\left(\frac{S_H^*}{N_H^*}\right) & 0 & \beta_{CH}\left(\frac{S_H^*}{N_C^*}\right) \\ 0 & 0 & 0 & 0 & 0 & 0 \\ 0 & 0 & 0 & 0 & 0 & 0 \\ 0 & 0 & 0 & 0 & 0 & 0 \\ 0 & \beta_{HC}\eta_{HA}\left(\frac{S_C^*}{N_H^*}\right) & \beta_{HC}\left(\frac{S_C^*}{N_H^*}\right) & 0 & 0 & \beta_{CC}\left(\frac{S_C^*}{N_C^*}\right) \\ 0 & 0 & 0 & 0 & 0 & 0 \end{bmatrix}$$

and

$$V = \begin{bmatrix} K_1 & 0 & 0 & 0 & 0 & 0 \\ -r\sigma_H & K_2 & 0 & 0 & 0 & 0 \\ -(1-r)\sigma_H & 0 & K_3 & 0 & 0 & 0 \\ 0 & 0 & -\phi_{HS} & K_4 & 0 & 0 \\ 0 & 0 & 0 & 0 & K_5 & 0 \\ 0 & 0 & 0 & 0 & -\sigma_C & K_6 \end{bmatrix},$$

where $K_1 = \sigma_H + \mu_H$, $K_2 = \gamma_{HA} + \mu_H + \delta_{HA}$, $K_3 = \phi_{HS} + \gamma_{HS} + \mu_H + \delta_{HS}$, $K_4 = \gamma_{HH} + \mu_H + \delta_{HH}$,

$K_5 = \sigma_C + \mu_C$, $K_6 = \gamma_C + \mu_C + \delta_C$, and $N_H^* = \Pi_H/\mu_H$. It is convenient to define $\mathbb{R}_{0M}$, the reproduction number of the model (2.1).

$$\begin{aligned}\mathbb{R}_{0M} &= \rho(\mathbb{F}\mathbb{V}^{-1}) \\ &= \frac{1}{2}\left\{\mathbb{R}_C + \mathbb{R}_H + \sqrt{\left(\mathbb{R}_C - \mathbb{R}_H\right)^2 + 4\left(\mathbb{R}_{H_AC} + \mathbb{R}_{H_SC}\right)}\right\},\end{aligned} \tag{3.2}$$

where

$$\mathbb{R}_H = \beta_{HH}\left(\frac{K_3K_4r\sigma_H\eta_{HA} + K_2(1-r)\sigma_H(K_4 + \eta_{HH}\phi_{HS})}{K_1K_2K_3K_4}\right),\ \mathbb{R}_C = \beta_{CC}\left(\frac{\sigma_C}{K_5K_6}\right),$$

$$\mathbb{R}_{H_AC} = \frac{\beta_{HC}\beta_{CH}r\sigma_H\eta_{HA}\sigma_C}{K_1K_2K_5K_6},\ \mathbb{R}_{H_SC} = \frac{\beta_{HC}\beta_{CH}(1-r)\sigma_H\sigma_C}{K_1K_3K_5K_6}. \tag{3.3}$$

The basic reproduction number $\mathbb{R}_{0M}$, of model (2.1), represents the average number of new cases (in humans or camels) generated by a typical infectious human or camel if introduced in a completely susceptible population of both humans and camels. The result below follows from Theorem 2 of [73].

Theorem 3.1. *The disease-free equilibrium of the model* (2.1) *is locally asymptotically stable if* $\mathbb{R}_{0M} < 1$*, and unstable if* $\mathbb{R}_{0M} > 1$.

The epidemiological implication of Theorem 3.1 is that a small influx of infected humans or camels in the well-mixed human-camel population (when $\mathbb{R}_{0M} < 1$) will not generate a significant MERS-CoV outbreak in the human-camel community if the initial number of infected humans or camels is small enough (i.e., in the basin of attraction of the aforementioned disease-free equilibrium). The terms in the expression for the basic reproduction number ($\mathbb{R}_{0M}$) of the model are epidemiologically interpreted below.

3.1.1. Epidemiological interpretation of $\mathbb{R}_{0M}$ for the model (2.1)

The terms in the expression for the basic reproduction number ($\mathbb{R}_{0M}$) for the model (2.1), given by (3.2), will be epidemiologically interpreted below. The expression for $\mathbb{R}_0$ contains four terms, namely $\mathbb{R}_H$, $\mathbb{R}_C$, $\mathbb{R}_{H_AC}$, and $\mathbb{R}_{H_SC}$. These terms will now be epidemiologically interpreted (it should be noted that $S_H^* = N_H^* = \Pi_H/\mu_H$ and $S_C^* = N_C^* = \Pi_C/\mu_C$).

Interpretation of $\mathbb{R}_H$

The quantity $\mathbb{R}_H$ is associated with the transmission dynamics of MERS-CoV between humans (only) in the community. It is convenient to re-write $\mathbb{R}_H$ in the following form:

$$\mathbb{R}_H = \mathbb{R}_{HA} + \mathbb{R}_{HS} + \mathbb{R}_{HH},$$

where

$$\mathbb{R}_{HA} = \frac{\beta_{HH}\eta_{HA}r\sigma_H}{K_1K_2},\ \mathbb{R}_{HS} = \frac{\beta_{HH}(1-r)\sigma_H}{K_1K_3},\ \mathbb{R}_{HH} = \frac{\beta_{HH}\eta_{HH}(1-r)\sigma_H\phi_{HS}}{K_1K_3K_4}. \tag{3.4}$$

That is, the quantity $\mathbb{R}_H$ is now expressed as the sum of the three constituent reproduction numbers for the average number of new cases generated by infectious humans in the asymptomatic ($\mathbb{R}_{HA}$), symptomatic ($\mathbb{R}_{HS}$), and hospitalized ($\mathbb{R}_{HH}$) compartments.

The terms in the constituent reproduction number $\mathbb{R}_{HA}$ can be expressed as follows. They are given by the product of the infection rate of susceptible humans with asymptomatically infectious humans near the DFE, given by $\left(\beta_{HH}\eta_{HA}\frac{S_H^*}{N_H^*}\right)$, the proportion that survived the exposed class and moved to the asymptomatically infectious class ($r\sigma_H/K_1$), and the average duration in the asymptomatically infectious class ($1/K_2$). Similarly, $\mathbb{R}_{HS}$ is the product of the infection rate of symptomatic humans near the DFE $\left(\beta_{HH}\frac{S_H^*}{N_H^*}\right)$, the proportion that survived the exposed class and moved to the symptomatically infectious class $\left(\frac{(1-r)\,\sigma_H}{K_1}\right)$, and the average duration in the symptomatically infectious class ($1/K_3$). Finally, $\mathbb{R}_{HH}$ is the product of the infection rate of hospitalized infectious humans near the DFE $\left(\beta_{HH}\eta_{HH}\frac{S_H^*}{N_H^*}\right)$, the proportion that survived the exposed class and moved to the symptomatically infectious class $\left(\frac{(1-r)\sigma_H}{K_1}\right)$, the proportion that survived the symptomatically infectious class and moved to the hospitalized class (ϕ_{HS}/K_3), and the average duration in the hospitalized class ($1/K_4$). The sum of the constituent reproduction numbers, $\mathbb{R}_{HA}$, $\mathbb{R}_{HS}$, and $\mathbb{R}_{HH}$, gives $\mathbb{R}_H$.

Interpretation of $\mathbb{R}_C$

The quantity $\mathbb{R}_C$ is associated with the transmission dynamics of MERS-CoV among camels (only) in the community. The terms in $\mathbb{R}_C$ represent the product of the infection rate of susceptible camels with infected camels near the DFE given by $\left(\beta_{CC}\frac{S_C^*}{N_C^*}\right)$, the proportion that survived the exposed class and moved to the infected camel class (σ_C/K_5), and the average duration in the infectious class ($1/K_6$).

Interpretation of $\mathbb{R}_{H_AC}$

This quantity is associated with the asymptomatically infectious humans camels asymptomatically infectious humans MERS-CoV transmission cycle. It is convenient to re-write it as:

$$\mathbb{R}_{H_AC} = \mathbb{R}_{h_{a_c}}\mathbb{R}_{CH},$$

where

$$\mathbb{R}_{h_{a_c}} = \left(\frac{\beta_{HC}\eta_{HA}r\sigma_H S_C^*}{K_1K_2N_H^*}\right) \text{and } \mathbb{R}_{CH} = \left(\frac{\beta_{CH}S_H^*}{K_5K_6N_C^*}\right)$$

with $\mathbb{R}_{h_{a_c}}$ representing a measure of MERS-CoV transmission from asymptomatically infectious humans to susceptible camels and $\mathbb{R}_{CH}$ accounting for MERS-CoV transmission from infectious camels

to susceptible humans. The quantity $\mathbb{R}_{h_{a_c}}$ represents the product of the infection rate of susceptible camels by asymptomatically infected humans $\left(\frac{\beta_{HC}\eta_{HA}S_C^*}{N_H^*}\right)$, the proportion of infected humans that survived the exposed class and moved to the asymptomatically infectious I_{HA} class, $\left(\frac{r\sigma_H}{K_1}\right)$, and the average duration in the I_{HA} class $\left(\frac{1}{K_2}\right)$. Similarly, the quantity $\mathbb{R}_{CH}$ is the product of the infection rate of susceptible humans by infectious camels, $\left(\frac{\beta_{CH}S_H^*}{N_C^*}\right)$, the proportion of infected camels that survived the exposed class and moved to the symptomatic class I_C, $\left(\frac{\sigma_C}{K_5}\right)$, and the average duration in the I_C class $\left(\frac{1}{K_6}\right)$.

Interpretation of $\mathbb{R}_{H_SC}$

This threshold quantity is associated with the symptomatic humans-camels-symptomatic humans MERS-CoV transmission cycle. It can be re-written as:

$$\mathbb{R}_{H_SC} = \mathbb{R}_{h_{s_c}}\mathbb{R}_{CH},$$

where $\mathbb{R}_{h_{s_c}}$ is a measure of MERS-CoV transmission from symptomatically infectious humans to susceptible camels and $\mathbb{R}_{CH}$ accounts for the MERS-CoV transmission from infectious camels to susceptible humans. Specifically, the quantity $\mathbb{R}_{h_{s_c}}$ is the product of the infection rate of susceptible camels by MERS-CoV symptomatic-infected humans $\left(\beta_{HC}\frac{S_C^*}{N_H^*}\right)$, the proportion of infected humans who survived the exposed class and moved to the symptomatically infectious I_{HS} class, $\left(\frac{(1-r)\sigma_H}{K_1}\right)$, and the average duration in the symptomatically infectious I_{HS} class, $\left(\frac{1}{K_3}\right)$. Similarly, the quantity $\mathbb{R}_{CH}$ is the product of the infection rate of susceptible humans by infectious camels, $\left(\frac{\beta_{CH}S_H^*}{N_C^*}\right)$, the proportion of infected camels that survived the exposed class and moved to the I_C class, $\left(\frac{\sigma_C}{K_5}\right)$, and the average duration in the I_C class $\left(\frac{1}{K_6}\right)$. The combinations of $\mathbb{R}_H$, $\mathbb{R}_C$, $\mathbb{R}_{H_AC}$, and $\mathbb{R}_{H_SC}$, in the way described in (3.2), gives $\mathbb{R}_{0M}$.

It should be mentioned that the square root in the expression for $\mathbb{R}_{0M}$, given by (3.2), is a consequence of the two generations (humans-camels-humans) needed to complete the cycles for generating $\mathbb{R}_{H_AC}$ and $\mathbb{R}_{H_SC}$. Furthermore, the numbers 1/2 and 4 in the expression (3.3) appeared because of the weighted averaging of the two modes (human-to-camel and camel-to-human) of MERS-CoV transmission [75]. It is also worth mentioning that, using the baseline values of the fixed and fitted parameters of the model (2.1) tabulated in Table 7, the value of the reproduction number ($\mathbb{R}_{0M}$) for MERS-CoV

transmission in the Kingdom of Saudi Arabia (using observed cumulative data from Week 13, 2013 to Week 9, 2014) is $\mathbb{R}_{0M} \approx 0.860$. Thus, since $\mathbb{R}_{0M}$ is less than one, it follows from the result of Theorem 3.1 that MERS-CoV can be effectively controlled in the Kingdom, and that such effective control is dependent on whether or not the initial sizes of the populations of infected humans or camels are small enough (i.e., if the initial numbers of infected hosts are in the basin of attraction of the disease-free equilibrium). Since $\mathbb{R}_{0M}$ is less than one for the Kingdom, our study shows that the prospect for MERS-CoV elimination in the Kingdom is promising provided the initial numbers of infected humans and camels are small enough.

The values of the fitted parameters of the model (2.1) can be used to determine the main drivers of the MERS-CoV pandemic in the Kingdom of Saudi Arabia, by computing the relative proportion of each of the fitted parameters in comparison to the total sum of these parameters). For instance, since the fitted value of the transmission rate for human to human is $\beta_{HH} = 0.114$ *per* week, and the sum of the values of all four fitted transmission rates is 0.842, it follows that, during the fitting period (i.e., from Week 13, 2013 to Week 42, 2013), human-to-human transmission accounts for about 14% (i.e., 0.114/0.842 expressed as a percentage) of all new MERS-CoV cases in the human-camel population of the Kingdom of Saudi Arabia. Table 2 depicts the proportion of new MERS-CoV cases generated by the various transmission pathways. It follows from this table that, during the fitting period, human-to-camel transmission accounts for 67% of all new MERS-CoV infections in the human-camel community within the Kingdom. Camel-to-camel transmission accounts for 16% of the new cases, while the camel-to-human transmission pathway accounts for only 3% of new cases.

Table 2. Contributions of various transmission pathways on the number of new MERS-CoV cases in the human-camel community of the Kingdom of Saudi Arabia, as measured by the relative proportion of the fitted values of the transmission rate parameters (β_{HH}, β_{CC}, β_{CH}, and β_{HC}) tabulated in Table 7.

Transmission rate parameter	Proportion of new infected cases
β_{HH}	14%
β_{CC}	16%
β_{CH}	3%
β_{HC}	67%

3.2. Data fitting and parameter estimation

The model (2.1) contains 23 parameters. While realistic values of most of them are available in the modeling literature (see Table 7), realistic values of the four contact rate parameters (namely β_{HH}, β_{CC}, β_{HC}, and β_{CH}) are unknown, and need to be estimated from observed data. To do so, we specifically fit the model (2.1) with the observed cumulative case data for MERS-CoV in the Kingdom of Saudi Arabia for the period from Week 13 of 2013 to Week 42 of 2013, and the segment of the data for the period from Week 43 of 2013 to Week 9 of 2014 is used to cross-validate the fitted model [6]. The least squares regression method is used to fit the model with the data [76–78]. This method entails finding the optimal parameter region that minimizes the root mean square difference between the predicted cumulative confirmed cases (generated from the model (2.1)) and the observed confirmed data [76–78].

The results obtained from the data fitting, depicted in Figure 4, show a reasonably good fit (and cross-validation). The estimated values of the four parameters (generated from the model fitting), and the associated 95% confidence intervals, are tabulated in Table 7.

Table 3. Baseline values of the four fitted parameters (and their confidence intervals) of the model (2.1).

Parameter	Fitted value (week^{-1})	95% Confidence Interval (week^{-1})
β_{HH}	0.114	[0.000–0.204]
β_{CC}	0.135	[0.126–0.143]
β_{CH}	0.023	[0.023–0.025]
β_{HC}	0.568	[0.000–0.999]

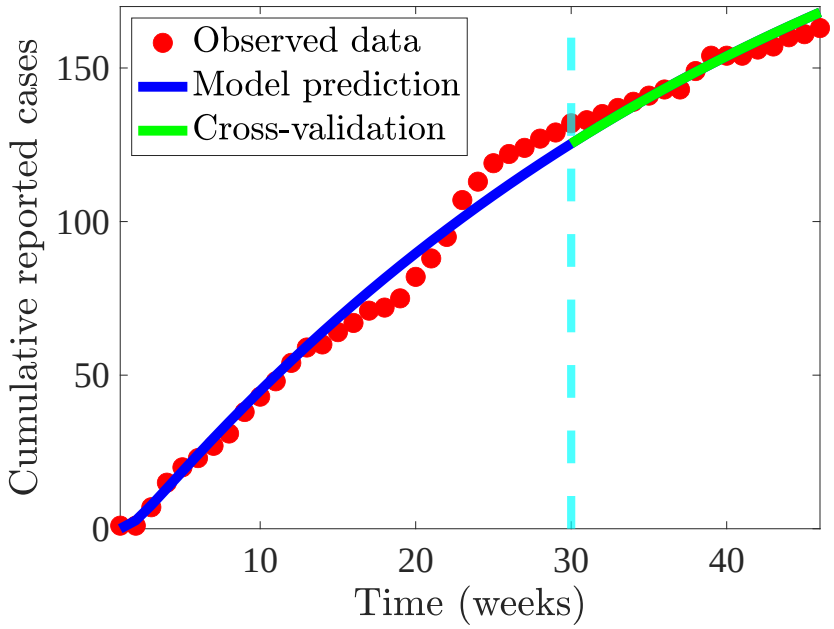

Figure 4. Data fitting of the model (2.1) using cumulative MERS-CoV new cases data for the Kingdom of Saudi Arabia from Week 13 of 2013 to Week 42 of 2013 (blue curve) and cross-validated using the segment of the data from Week 43 of 2013 to Week 9 of 2014 (green curve) [6]. The baseline values and the values of the four fitted parameters in Table 7 and Figure 1 were used in generating this figure.

3.3. Global parameter sensitivity analysis

The model (2.1) contains 23 parameters, and sensitivity analysis will be conducted to determine the parameters that have the most influence on the transmission dynamics of the disease. The global parameter sensitivity analysis entails using the Latin hypercube sampling (LHS) approach and partial rank correlation coefficients (PRCCs) [79–83] to identify the parameters of the model that have the most influence on the chosen response function, $\mathbb{R}_0$ [79, 80, 84, 85]. In order to carry out the sensitivity

analysis, a range (lower and upper bound) and distribution must first be established for each parameter of the model. Since the values of the demographic parameters for humans and camels, namely Π_H, Π_C, μ_H, and μ_C, are realistically known from census data [28,47,86–88], these four parameters are not included in the sensitivity analysis. Parameters with high PRCC values close to -1 or +1 are said to be highly correlated with the response function [12, 89]. Those with negative (positive) PRCC values are said to be negatively (positively) correlated with the response function ($\mathbb{R}_{0M}$) [12, 89]. The baseline values and ranges of the parameters of the model (2.1) needed for the sensitivity analysis are tabulated in Table 4. The control basic reproduction number, $\mathbb{R}_{0M}$, is chosen as the response function. The results obtained for the global sensitivity analysis of the model (2.1), with respect to the response function $\mathbb{R}_{0M}$, are depicted in Figure 5 (and also tabulated in Table 4). It follows from Figure 5 and Table 4 that the parameters that have the most effect on the response function ($\mathbb{R}_{0M}$) are:

(a) the rate at which camels recover from infection (γ_C, with a PRCC value -0.980),

(b) the transmission rate from infected camels to susceptible camels (β_{CC}, with a PRCC value $+0.921$),

(c) the transmission rate from infected humans to susceptible camels (β_{HC}, with a PRCC value $+0.569$).

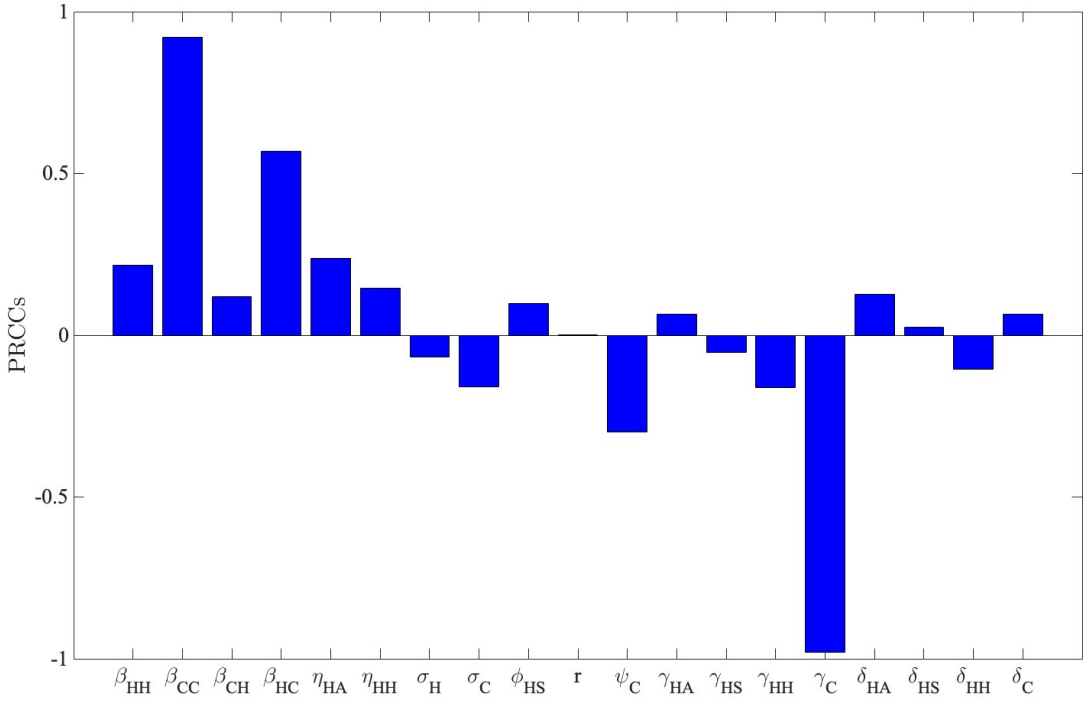

Figure 5. Partial rank correlation coefficients (PRCCs) of the parameters in the expression of the basic reproduction number $\mathbb{R}_{0M}$ of the model (2.1). The baseline values of the parameters used in generating the PRCC values are as given in Table 7.

Table 4. PRCC values of the parameters (19 of 23) of the model (2.1), with $\mathbb{R}_{0M}$ chosen as the response function. Parameters with PRCCs ≥ 0.5 in magnitude are considered to be highly correlated with the response function, and are highlighted in bold font.

Parameter	Baseline value	Range	PRCC
β_{HH}	0.114	0.091–0.137	0.216
β_{CC}	0.135	0.108–0.163	**0.921**
β_{CH}	0.023	0.018–0.027	0.119
β_{HC}	0.568	0.454–0.682	**0.569**
η_{HA}	0.500	0.400–0.600	0.238
η_{HH}	0.100	0.080–0.120	0.144
σ_H	1.400	1.120–1.680	-0.067
σ_C	2	1.600–2.400	-0.160
ϕ_{HS}	1.750	1.400–2.100	0.098
r	0.251	0.200–0.301	0.000
ψ_C	0.200	0.160–0.240	-0.299
γ_{HA}	1	0.800–1.200	0.065
γ_{HS}	0.583	0.466–0.699	-0.053
γ_{HH}	0.388	0.311–0.466	-0.162
γ_C	0.166	0.133–0.200	**-0.980**
δ_{HA}	3.50×10^{-7}	2.80×10^{-7}–4.20×10^{-7}	0.125
δ_{HS}	3.37×10^{-6}	2.69×10^{-6}–4.04×10^{-6}	0.024
δ_{HH}	3.37×10^{-6}	2.69×10^{-6}–4.04×10^{-6}	-0.104
δ_C	3.60×10^{-7}	2.88×10^{-7}–4.32×10^{-7}	0.065

Thus, based on the parameter values used in the sensitivity analysis and the data used to fit the model (2.1), we identified the top-three parameters that have the highest influence on the dynamics and burden of MERS-CoV (as measured by the changes in the basic reproduction number, $\mathbb{R}_{0M}$) in the Kingdom of Saudi Arabia. Since the recovery rate parameter for camels (γ_C) has the highest negative correlation with the response function, it follows that control and mitigation strategies (such as isolation and treatment of infectious camels with highly effective antiviral drugs) that increase the recovery rates strategy will reduce the response function (and, consequently, reduce the burden of the disease in the community). Furthermore, the transmission rate parameter from infected camels to susceptible camels (β_{CC}) and from infected humans to susceptible camels (β_{HC}) are highly positively correlated with the response function. Hence, the implementation of control and mitigation strategies that reduce the values of these transmission parameters, such as the quarantine of susceptible camels suspected of being exposed to MERS-CoV and isolation of camels with confirmed symptoms of the disease, will reduce the disease burden in the human and camel populations. Furthermore, these parameters can be reduced by the use of effective face masks by humans who have frequent contacts with camels or the quarantine and isolation of humans suspected of being exposed or those with confirmed symptoms, respectively. In summary, the global sensitivity analysis carried out in this section identified three parameters that have the highest influence on the MERS-CoV transmission dynamics in the KSA.

Consequently, control strategies that target these parameters (as described above) will be most effective in reducing the disease burden (and/or eliminating the disease) in the Kingdom.

4. Extended model (2.1) with public health interventions

As discussed in Section 1, numerous public health control and mitigation strategies are being implemented or proposed in an attempt to effectively curtail the spread of the MERS-CoV pandemic in the human and camel populations. In particular, non-pharmaceutical interventions, such as the use of face masks (to prevent human-to-human or human-to-camel or camel-to-human transmission), quarantine and isolation of suspected humans (camels) and those with clinical symptoms of the disease, are deployed or proposed in an attempt to effectively control the spread and burden of MERS-CoV in the human and camel populations [18, 40, 42]. Similarly, pharmaceutical interventions, such as the vaccination of humans and/or camels are being proposed as possible future additions to the armory of interventions against the MERS-CoV pandemic [49–51, 53, 57]. In this section, the basic model (2.1) developed in Section 2.1 will be extended to allow for the assessment of the population-level impact of public health intervention (pharmaceutical and non-pharmaceutical), notably face mask usage and the vaccination of both humans and camels. The extended model is formulated below.

4.1. Formulation of the extended model

The extended model to be formulated in this section is based on extending the basic model (2.1) to include the effect of face mask usage (by humans) and vaccination (of both humans and camels). In order to incorporate vaccination and the use of face masks, two new state variables will be added to the basic model (2.1). Specifically, we let $V_H(t)$ represent the total number of susceptible humans vaccinated against MERS-CoV at time t. Similarly, let $V_C(t)$ be the total number of susceptible camels vaccinated against MERS-CoV at time t. Furthermore, in order to incorporate the use of the face mask among humans, we re-scaled the transmission rate parameter from infectious humans to susceptible humans, β_{HH}, by $\beta_{HH}(1 - \varepsilon_{mh}c_{mh})$, where $0 \leq \varepsilon_{mh} \leq 1$ represents the efficacy (effectiveness) of the face mask to prevent transmission or acquisition of MERS-CoV infection (from infectious humans to susceptible humans) and $0 \leq c_{mh} \leq 1$ accounts for the compliance (or coverage) of face mask usage by the members of the public. Similarly, in order to incorporate the use of the face mask by humans who have close contact with camels, we re-scaled the transmission rate parameter from infectious camels to susceptible humans, β_{CH}, by $\beta_{CH}(1 - \varepsilon_{mc}c_{mc})$; where $0 \leq \varepsilon_{mc} \leq 1$ represents the efficacy of the face mask to prevent transmission or acquisition of MERS-CoV infection by infectious camels to susceptible humans, and $0 \leq c_{mc} \leq 1$ measures the masking compliance by individuals who have close contact with camels. Finally, in order to incorporate the use of the face mask by infected humans who have close contact with susceptible camels, we re-scaled the transmission rate parameter from infectious humans to susceptible camels, β_{HC}, by $\beta_{HC}(1 - \varepsilon_{mc}c_{mc})$, where $0 \leq \varepsilon_{mc} \leq 1$ represents the efficacy of the face mask to prevent transmission of infection and $0 \leq c_{mc} \leq 1$ accounts for the compliance in its usage.

It follows, based on the above definitions and assumptions, that the equation for the rate of change of the susceptible human population is now given by:

$$\dot{S}_H = \Pi_H + \omega_{VH}V_H - (\lambda_H + \lambda_{CH} + \xi_{VH} + \mu_H)S_H, \tag{4.1}$$

where the parameter Π_H is the recruitment rate of humans, ω_{VH} is the waning rate of the vaccine, ξ_{VH} is the vaccination rate of humans, μ_H is the natural death rate of humans, and λ_H and λ_{CH} are the human-to-human transmission rate and the camel-to-human transmission rate now defined, respectively (note that the parameters β_{HH}, η_{HA}, η_{HH}, and β_{CH} are as defined above and in Section 2.1):

$$\begin{aligned} \lambda_H &= (1-\varepsilon_{mh}c_{mh})\left[\frac{\beta_{HH}\left(\eta_{HA}I_{HA}+I_{HS}+\eta_{HH}I_{HH}\right)}{N_H}\right], \\ \lambda_{CH} &= [\beta_{CH}(1-\varepsilon_{mc}c_{mc})]\left(\frac{I_C}{N_C}\right). \end{aligned} \tag{4.2}$$

Similarly, the rate of change of the vaccinated human population is given by:

$$\dot{V}_H = \xi_{VH}S_H - \omega_{VH}V_H - (1-\varepsilon_{VH})(\lambda_H+\lambda_{CH})V_H - \mu_H V_H, \tag{4.3}$$

where ξ_{VH} is the vaccination rate, ω_{VH} is the vaccine waning rate, and $0 < \varepsilon_{VH} < 1$ is the average protective efficacy of the vaccine to prevent vaccinated susceptible humans from acquiring MERS-CoV infection.

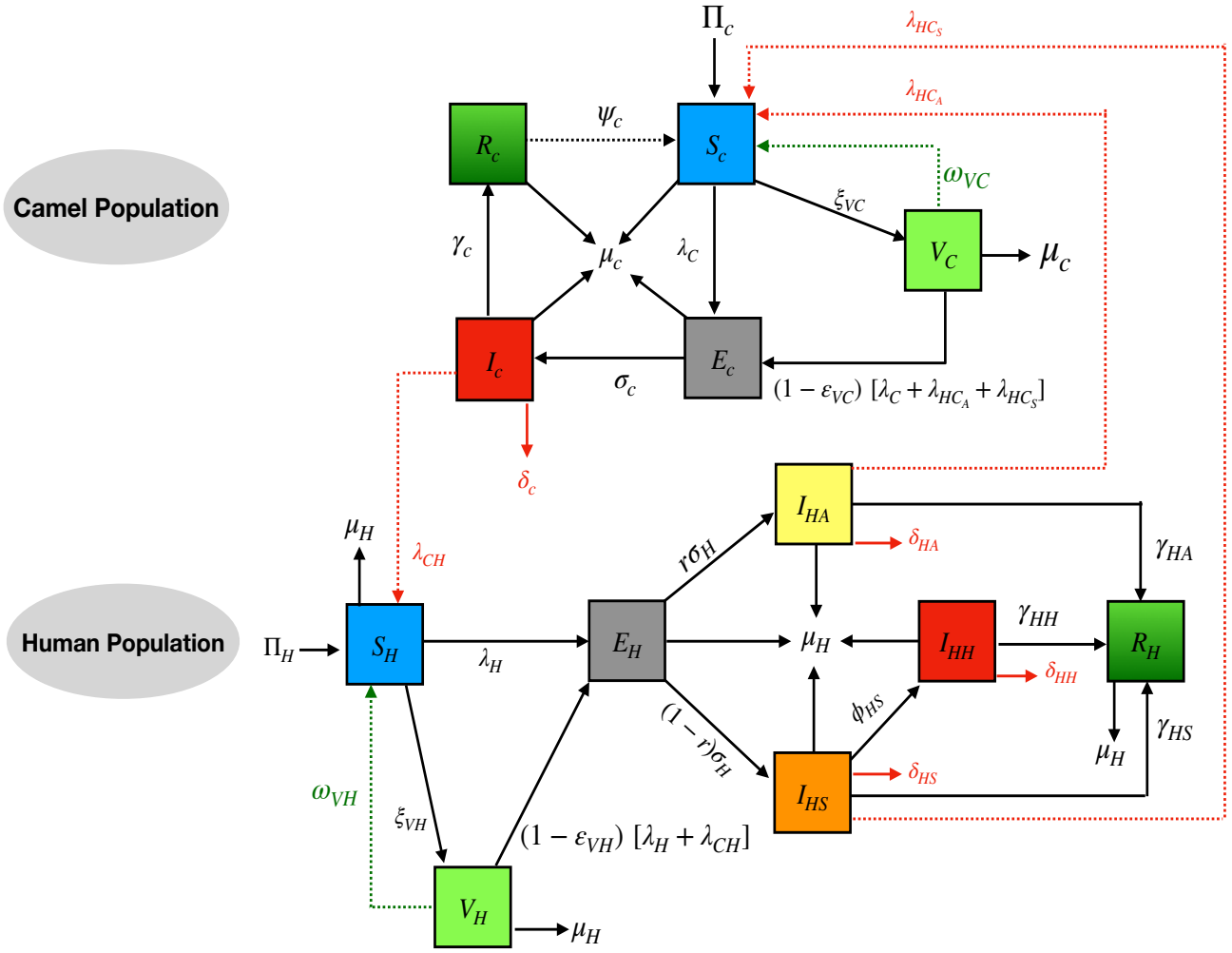

Figure 6. Flow diagram of the extended model (4.6), with the infection rates $\lambda_H, \lambda_C, \lambda_{CH}, \lambda_{HC_A}$, and λ_{HC_S} as defined in Eqs (4.2) and (4.5) [4].

Table 5. A Description of the state variables of the original model (2.1) and the extended model (4.6).

State variable	Description
S_H	Population of susceptible humans
V_H	Population of vaccinated humans
E_H	Population of exposed (newly infected) humans
I_{HA}	Population of asymptomatically infectious humans
I_{HS}	Population of symptomatically infectious humans
I_{HH}	Population of hospitalized infectious humans
R_H	Population of recovered humans
S_C	Population of susceptible camels
V_C	Population of vaccinated camels
E_C	Population of exposed (newly infected) camels
I_C	Population of symptomatically infectious camels
R_C	Population of recovered camels

Furthermore, the rate of change of the population of vaccinated camels is given by:

$$\dot{V}_C = \xi_{VC} S_C - \omega_{VC} V_C - (1 - \varepsilon_{VC})(\lambda_C + \lambda_{HC_A} + \lambda_{HC_S}) V_C - \mu_C V_C, \tag{4.4}$$

where ξ_{VC} is the vaccination rate of camels, ω_{VC} is the vaccine waning rate for vaccinated camels, $0 < \varepsilon_{VC} < 1$ is the average protective efficacy of the vaccine to prevent susceptible camels from acquiring MERS-CoV infection, μ_C is the natural death rate of camels, and the infection rates λ_C, λ_{HC_A}, and λ_{HC_S} (for the camel-to-camel transmission, asymptomatic-human-to-camel transmission, and symptomatic-human-to-camel transmission, respectively) are now given, respectively, by:

$$\begin{aligned} \lambda_C &= (\beta_{CC})\left(\frac{I_C}{N_C}\right), \\ \lambda_{HC_A} &= [\beta_{HC}(1 - \varepsilon_{mc} c_{mc})]\left(\frac{\eta_{HA} I_{HA}}{N_H}\right), \\ \lambda_{HC_S} &= [\beta_{HC}(1 - \varepsilon_{mc} c_{mc})]\left(\frac{I_{HS}}{N_H}\right). \end{aligned} \tag{4.5}$$

It follows, based on the above derivations and assumptions, that the extended MERS-CoV model with public health interventions is given by the original (basic) model (2.1), but with the equation for the rate of change of the susceptible population now replaced by Eq (4.1), together with Eqs (4.3) and (4.4). In other words, the extended model for the transmission dynamic of MERS-CoV in a human-camel population, that incorporates vaccination of humans and camels and the use of face masks by humans, is given by the following deterministic system of nonlinear differential equations. The flow diagram of the extended model is depicted in Figure 6, and the state variables and parameters of the

extended model (4.6) are described in Tables 5 and 6, respectively [4].

$$
\begin{aligned}
\dot{S}_H &= \Pi_H + \omega_{VH} V_H - (\lambda_H + \lambda_{CH} + \xi_{VH} + \mu_H) S_H, \\
\dot{V}_H &= \xi_{VH} S_H - \omega_{VH} V_H - (1 - \varepsilon_{VH})(\lambda_H + \lambda_{CH}) V_H - \mu_H V_H, \\
\dot{E}_H &= (\lambda_H + \lambda_{CH}) S_H + (1 - \varepsilon_{VH})(\lambda_H + \lambda_{CH}) V_H - (\sigma_H + \mu_H) E_H, \\
\dot{I}_{HA} &= r\sigma_H E_H - (\gamma_{HA} + \mu_H + \delta_{HA}) I_{HA}, \\
\dot{I}_{HS} &= (1 - r)\,\sigma_H E_H - (\phi_{HS} + \gamma_{HS} + \mu_H + \delta_{HS}) I_{HS}, \\
\dot{I}_{HH} &= \phi_{HS} I_{HS} - (\gamma_{HH} + \mu_H + \delta_{HH}) I_{HH}, \\
\dot{R}_H &= \gamma_{HA} I_{HA} + \gamma_{HS} I_{HS} + \gamma_{HH} I_{HH} - \mu_H R_H, \\
\dot{S}_C &= \Pi_C + \psi_C R_C + \omega_{VC} V_C - (\lambda_C + \lambda_{HC_A} + \lambda_{HC_S} + \xi_{VC} + \mu_C) S_C, \\
\dot{V}_C &= \xi_{VC} S_C - \omega_{VC} V_C - (1 - \varepsilon_{VC})(\lambda_C + \lambda_{HC_A} + \lambda_{HC_S}) V_C - \mu_C V_C, \\
\dot{E}_C &= (\lambda_C + \lambda_{HC_A} + \lambda_{HC_S}) S_C + (1 - \varepsilon_{VC})(\lambda_C + \lambda_{HC_A} + \lambda_{HC_S}) V_C - (\sigma_C + \mu_C) E_C, \\
\dot{I}_C &= \sigma_C E_C - (\gamma_C + \mu_C + \delta_C) I_C, \\
\dot{R}_C &= \gamma_C I_C - (\psi_C + \mu_C) R_C,
\end{aligned}
\tag{4.6}
$$

where the rates for the human-to-human (λ_H), camel-to-camel (λ_C), camel-to-human (λ_{CH}), asymptomatically-infectious-human-to-camel (λ_{HC_A}), and symptomatically-infectious-human-to-camel (λ_{HC_S}) transmission are given in (4.2) and (4.5).

Some of the additional assumptions made in the formulation of the extended model (4.6) are:

(i) Vaccinated susceptible humans (in the V_H class) are assumed to have received the full required vaccine doses and that enough time has elapsed for the body to develop vaccine-derived immunity. Similarly, vaccinated susceptible camels (in the V_C class) are assumed to have received the full required vaccine doses.
(ii) The vaccines (for both humans and camels) are assumed to be imperfect. Further, the protective efficacy of each of the two vaccines is assumed to wane with time.

The following result can also be proved using the approach used to prove Theorem (2.1).

Theorem 4.1. *Consider the closed sets*

$$
\mathbb{D}_{H_E} = \left\{ (S_H, V_H, E_H, I_{HA}, I_{HS}, I_{HH}, R_H) \in \mathbb{R}_+^7 \right\} \text{ and } \mathbb{D}_{C_E} = \left\{ (S_C, V_C, E_C, I_C, R_C) \in \mathbb{R}_+^5 \right\}.
$$

The region $\mathbb{D}_{\mathbb{E}} = \mathbb{D}_{H_E} \cup \mathbb{D}_{C_E}$ *is positively invariant and attracting with respect to the extended model* (4.6).

Table 6. Description of the parameters of the original model (2.1) and the extended model (4.6).

Parameter	Description
Π_H	Recruitment (birth or immigration) rate of humans into the community
Π_C	Recruitment (birth or importation) rate of camels into the community
μ_H	Natural death rate for humans
μ_C	Natural death rate for camels
β_{HH}	Transmission rate from infected humans to susceptible humans
β_{CC}	Transmission rate from infected camels to susceptible camels
β_{HC}	Transmission rate from infected humans to susceptible camels
β_{CH}	Transmission rate from infected camels to susceptible humans
η_{HA}	Modification parameter for the infectiousness of asymptomatically infectious humans, in comparison to the infectiousness of symptomatic humans
η_{HH}	Modification parameter for the infectiousness of hospitalized humans, in comparison to the infectiousness of symptomatic humans
σ_H	Rate at which exposed (newly infected) humans become infectious
σ_C	Rate at which exposed (newly infected) camels become infectious
ϕ_{HS}	Hospitalization rate of symptomatic infectious humans
r	Proportion of newly infectious humans who do not show clinical symptoms of the disease
$1-r$	Proportion of newly infectious humans who show clinical symptoms of the disease
ψ_C	Rate of loss of natural immunity for camels
γ_{HA}	Recovery rate for asymptomatically infectious humans
γ_{HS}	Recovery rate for symptomatically infectious humans
γ_{HH}	Recovery rate for hospitalized infectious humans
γ_C	Recovery rate for infectious camels
δ_{HA}	Disease-induced mortality rate for asymptomatically-infectious humans
δ_{HS}	Disease-induced mortality rate for symptomatically infectious humans
δ_{HH}	Disease-induced mortality rate for hospitalized humans
δ_C	Disease-induced mortality rate for camels
ξ_{VH}	Vaccination rate for humans
ω_{VH}	Vaccine waning rate for vaccinated humans
ε_{VH}	Efficacy of the vaccine to prevent susceptible humans from acquiring infection
ε_{mh}	Efficacy of face mask to prevent disease transmission from infectious humans to susceptible humans
ε_{mc}	Efficacy of face mask to prevent disease transmission from infectious camels to susceptible humans
c_{mh}	Face mask coverage (compliance) by humans to prevent human-to-human transmission
c_{mc}	Face mask coverage (compliance) for humans who have frequent close contact with camels
ξ_{VC}	Vaccination rate for camels
ω_{VC}	Vaccine waning rate for vaccinated camels
ε_{VC}	Efficacy of the vaccine to prevent susceptible camels from acquiring infection

Table 7. Baseline values of the fixed and estimated parameters of the original model (2.1) and the extended model (4.6).

Parameter	Baseline value (week^{-1})	Reference
Π_H	191	[86, 87]
Π_C	14	[47, 88]
μ_H	5.21×10^{-6}	[86, 87]
μ_C	9.78×10^{-6}	[28, 88]
β_{HH}	0.114	Fitted
β_{CC}	0.135	Fitted
β_{CH}	0.023	Fitted
β_{HC}	0.568	Fitted
η_{HA}	0.5 (dimensionless)	Assumed
η_{HH}	0.1 (dimensionless)	Assumed
σ_H	1.400	[59, 90, 91]
σ_C	2	[63]
ϕ_{HS}	1.750	[15, 90]
r	0.251 (dimensionless)	[45]
$1 - r$	0.749 (dimensionless)	[45]
ψ_C	0.2	[26]
γ_{HA}	1	[15]
γ_{HS}	0.583	[90]
γ_{HH}	0.388	[28]
γ_C	0.166	[92]
δ_{HA}	3.5×10^{-7}	Assumed
δ_{HS}	3.37×10^{-6}	Adapted from [7, 87]
δ_{HH}	3.37×10^{-6}	Adapted from [7, 87]
δ_C	3.6×10^{-7}	Assumed
ξ_{VH}	2.8×10^{-6}	[93]
ω_{VH}	0.027	[94]
ξ_{VC}	1×10^{-3}	Assumed
ω_{VC}	0.027	[94]

4.2. Theoretical analysis of the extended model: stability of DFE

The unique DFE of the extended model (4.6) is given by:

$$\begin{aligned}\mathbb{E}_{0v} &= (S_H^*, V_H^*, E_H^*, I_{HA}^*, I_{HS}^*, I_{HH}^*, R_H^*, S_C^*, V_C^*, E_C^*, I_C^*, R_C^*)\\ &= \left(\frac{\Pi_H(\omega_{VH}+\mu_H)}{\mu_H(\omega_{VH}+\xi_{VH}+\mu_H)}, \frac{\Pi_H\xi_{VH}}{\mu_H(\omega_{VH}+\xi_{VH}+\mu_H)}, 0, 0, 0, 0, 0,\right.\\ &\left.\frac{\Pi_C(\omega_{VC}+\mu_C)}{\mu_C(\omega_{VC}+\xi_{VC}+\mu_C)}, \frac{\Pi_C\xi_{VC}}{\mu_C(\omega_{VC}+\xi_{VC}+\mu_C)}, 0, 0, 0\right).\end{aligned} \tag{4.7}$$

Here, too, the linear asymptotic stability of the DFE will be explored using the next generation operator method (used in Section 3). Specifically, the associated non-negative matrix (F_v) of the new infection terms is given by:

$$F_v = \begin{bmatrix} 0 & f_1 & f_2 & f_3 & 0 & f_4 \\ 0 & 0 & 0 & 0 & 0 & 0 \\ 0 & 0 & 0 & 0 & 0 & 0 \\ 0 & 0 & 0 & 0 & 0 & 0 \\ 0 & g_1 & g_2 & 0 & 0 & g_3 \\ 0 & 0 & 0 & 0 & 0 & 0 \end{bmatrix}$$

where

$f_1 = (1-\varepsilon_{mh}c_{mh})\beta_{HH}\eta_{HA}\left[\frac{S_H^* + (1-\varepsilon_{VH})V_H^*}{N_H^*}\right]$, $f_2 = (1-\varepsilon_{mh}c_{mh})\beta_{HH}\left[\frac{S_H^* + (1-\varepsilon_{VH})V_H^*}{N_H^*}\right]$,

$f_3 = (1-\varepsilon_{mh}c_{mh})\beta_{HH}\eta_{HH}\left[\frac{S_H^* + (1-\varepsilon_{VH})V_H^*}{N_H^*}\right]$, $f_4 = (1-\varepsilon_{mc}c_{mc})\beta_{CH}\left[\frac{S_H^* + (1-\varepsilon_{VH})V_H^*}{N_C^*}\right]$,

$g_1 = (1-\varepsilon_{mc}c_{mc})\beta_{HC}\eta_{HA}\left[\frac{S_C^* + (1-\varepsilon_{VC})V_C^*}{N_H^*}\right]$, $g_2 = (1-\varepsilon_{mc}c_{mc})\beta_{HC}\left[\frac{S_C^* + (1-\varepsilon_{VC})V_C^*}{N_H^*}\right]$

and $g_3 = \beta_{CC}\left[\frac{S_C^* + (1-\varepsilon_{VC})V_C^*}{N_C^*}\right]$. It should be noted that the proportion of humans vaccinated at the disease-free steady-state is given by $\frac{V_H^*}{N_H^*} = \frac{\xi_{VH}}{\omega_{VH}+\xi_{VH}+\mu_H} = f_{VH}$. Similarly, the proportion of camels vaccinated at the disease-free steady-state is $\frac{V_C^*}{N_C^*} = \frac{\xi_{VC}}{\omega_{VC}+\xi_{VC}+\mu_C} = f_{VC}$.

Similarly, the matrix (V) of the linear transition terms (as defined in Section 3) is given by:

$$V = \begin{bmatrix} K_1 & 0 & 0 & 0 & 0 & 0 \\ -r\sigma_H & K_2 & 0 & 0 & 0 & 0 \\ -(1-r)\sigma_H & 0 & K_3 & 0 & 0 & 0 \\ 0 & 0 & -\phi_{HS} & K_4 & 0 & 0 \\ 0 & 0 & 0 & 0 & K_5 & 0 \\ 0 & 0 & 0 & 0 & -\sigma_C & K_6 \end{bmatrix}$$

where $K_i\,(i = 1, \cdots, 6)$ are as defined in Section 3. It follows that the control reproduction number of the extended model (4.6), denoted by $\mathbb{R}_{CM}$, is given by:

$$\begin{aligned} \mathbb{R}_{CM} &= \rho(\mathbb{F}\mathbb{V}^{-1}) \\ &= \frac{1}{2}\left[\mathbb{R}_{CC} + \mathbb{R}_{HH} + \sqrt{\left(\mathbb{R}_{CC} - \mathbb{R}_{HH}\right)^2 + 4\,\mathbb{R}_{CH}\mathbb{R}_{HC}}\right] \end{aligned} \tag{4.8}$$

where (following the approach in [95]), $\mathbb{R}_{CC}, \mathbb{R}_{HH}, \mathbb{R}_{CH}$, and $\mathbb{R}_{HC}$ are given by:

$$\mathbb{R}_{CC} = \frac{K_1K_2K_3K_4\sigma_C g_3}{\prod_{i=1}^{6} K_i}, \ \mathbb{R}_{HH} = \frac{K_5K_6\sigma_H[rf_1K_3K_4 + (1-r)K_2(f_2K_4 + f_3\phi_{HS})]}{\prod_{i=1}^{6} K_i},$$
$$\mathbb{R}_{CH} = \frac{\sigma_C K_1K_2K_3K_4 f_4}{\prod_{i=1}^{6} K_i}, \ \mathbb{R}_{HC} = \frac{\sigma_H K_4K_5K_6[rg_1K_3 + (1-r)g_2K_2]}{\prod_{i=1}^{6} K_i}. \tag{4.9}$$

The quantity $\mathbb{R}_{CM}$ is the control reproduction number of the extended model (4.6), and it measures the average number of new MERS-CoV cases (in humans or camels) generated by a typical infectious human or camel if introduced in a human-camel population where a vaccination program (of both humans and camels, using imperfect human and camel vaccines) is implemented, and a certain proportion of humans wear face masks in public (to prevent human-to-human transmission) and when having direct contact with camels (to prevent human-to-camel or camel-to-human transmission). The result below follows from Theorem 2 of [73].

Theorem 4.2. *The disease-free equilibrium* ($\mathbb{E}_{0v}$) *of the vaccination model* (4.6) *is locally asymptotically stable if* $\mathbb{R}_{CM} < 1$*, and unstable if* $\mathbb{R}_{CM} > 1$.

The epidemiological implication of Theorem 4.2 is that a small influx of infected humans or camels in the well-mixed human-camel population (when $\mathbb{R}_{CM} < 1$) will not generate a significant MERS-CoV outbreak in the human-camel community if the initial number of infected humans or camels is small enough (i.e., in the basin of attraction of the aforementioned disease-free equilibrium).

5. Numerical simulations

The extended model (4.6) will now be simulated to assess the population-level impact of pharmaceutical and non-pharmaceutical intervention strategies, such as the use of face masks (by humans in public or when in close proximity with camels) and vaccination (of both humans and camels), on the transmission dynamics and control of MERS-CoV in the Kingdom of Saudi Arabia. Unless otherwise noted, the simulations will be carried out using the baseline values of the fixed and fitted parameters given in Table 7. The following three intervention scenarios will be simulated:

(a) **Scenario 1 (face mask as a sole intervention):** Thr use of face masks worn by individuals having close contact with camels is implemented as the sole intervention in the community.

(b) **Scenario 2 (vaccinating humans or camels as a sole intervention):**

  (2a) The vaccination of humans as the sole intervention is implemented in the community.
  (2b) The vaccination of camels as the sole intervention is implemented in the community.

(c) **Scenario 3 (combined mask-vaccination (hybrid) strategy)**: The vaccination (of both humans and camels) and the use of face masks by humans in public or when in close proximity with camels is administered as the main intervention in the community.

Most of the simulations to be carried out are for the period between May 1, 2023 (considered as Day 1 of our simulations) and April 30, 2024. Further, for simulation purposes, the initial conditions of the model will be chosen based on the initial cumulative number of MERS-CoV cases (2196) and mortality (855) in humans, as well as the cumulative number of cases in camels (977), in the Kingdom of Saudi Arabia recorded on May 1, 2023 (considered as Day 1 of the simulations) [7,96]). The aforementioned three simulation scenarios are briefly discussed below.

5.1. Scenario 1: The effect of face masks as the sole public health intervention against human-to-camel and camel-to-human transmission

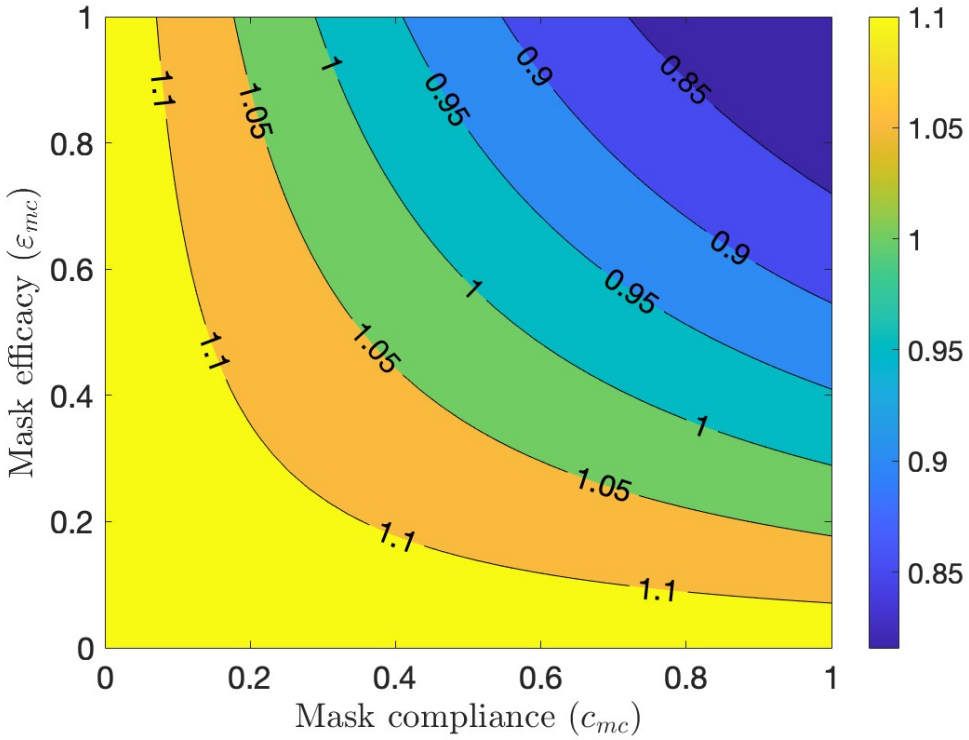

Figure 7. Simulations of the extended model (4.6) to assess the effect of the use of face masks by humans within close proximity to camels as the sole public health intervention (Scenario 1), depicting contour plots of the associated control reproduction number ($\widetilde{\mathbb{R}}_{CM}$) of the extended model (4.6), as a function of mask efficacy (ε_{mc}) and compliance (c_{mc}). The other parameter values used to generate the contour plots are as given in Table 7, with $\xi_{VH} = \varepsilon_{VH} = \omega_{VH} = \xi_{VC} = \varepsilon_{VC} = \omega_{VC} = \varepsilon_{mh} = c_{mh} = 0$ and, now, $\beta_{CH} = 0.223$.

To assess the impact of face mask use as a sole intervention (where the masks are worn by humans when they come in close proximity with camels only) on the transmission dynamics and control of MERS-CoV in the KSA, the extended model (4.6) is simulated for the special case without vaccination (i.e., $\xi_{VH} = \varepsilon_{VH} = \omega_{VH} = \xi_{VC} = \varepsilon_{VC} = \omega_{VC} = 0$) and humans do not wear face masks in public (i.e., $\varepsilon_{mh} = c_{mh} = 0$). The simulation results obtained are illustrated in the form of contour plots of the associated control reproduction number, denoted by $\widetilde{\mathbb{R}}_{CM_{mc}}$ ($\widetilde{\mathbb{R}}_{CM_{mc}} = \mathbb{R}_{CM}|_{\xi_{VH}=\varepsilon_{VH}=\omega_{VH}=\xi_{VC}=\varepsilon_{VC}=\omega_{VC}=\varepsilon_{mh}=c_{mh}=0}$),

as a function of face mask efficacy (ε_{mc}) and coverage (c_{mc}), depicted in Figure 7. This figure shows that the associated control reproduction number $\widetilde{\mathbb{R}}_{CM_{mc}}$ decreases with increasing values of the mask efficacy and compliance, and that $\widetilde{\mathbb{R}}_{CM_{mc}}$ lies in the range $\widetilde{\mathbb{R}}_{CM_{mc}} \in [0.85, 1.1]$ (suggesting that the use of face masks as a sole intervention can lead to the elimination of the disease in the population, depending on the efficacy of, and the compliance in using, face masks in the community. For example, this figure shows that if surgical masks (with an estimated efficacy of about 70% [93, 97]) is prioritized, the disease can be effectively controlled or eliminated (in both the human and camel populations) if at least 45% of the human population consistently wear such masks whenever they are within close proximity to camels. This result is illustrated, by simulating the extended model with mask efficacy and compliance set at 70% and 45%, respectively (and other parameter values chosen such that the associated reproduction number of the model, denoted by $\widetilde{\mathbb{R}}_{CM} <$, is less than one), showing convergence of multiple initial conditions to the disease-free equilibrium (see Figure (8); which suggests disease elimination in about 300 days).

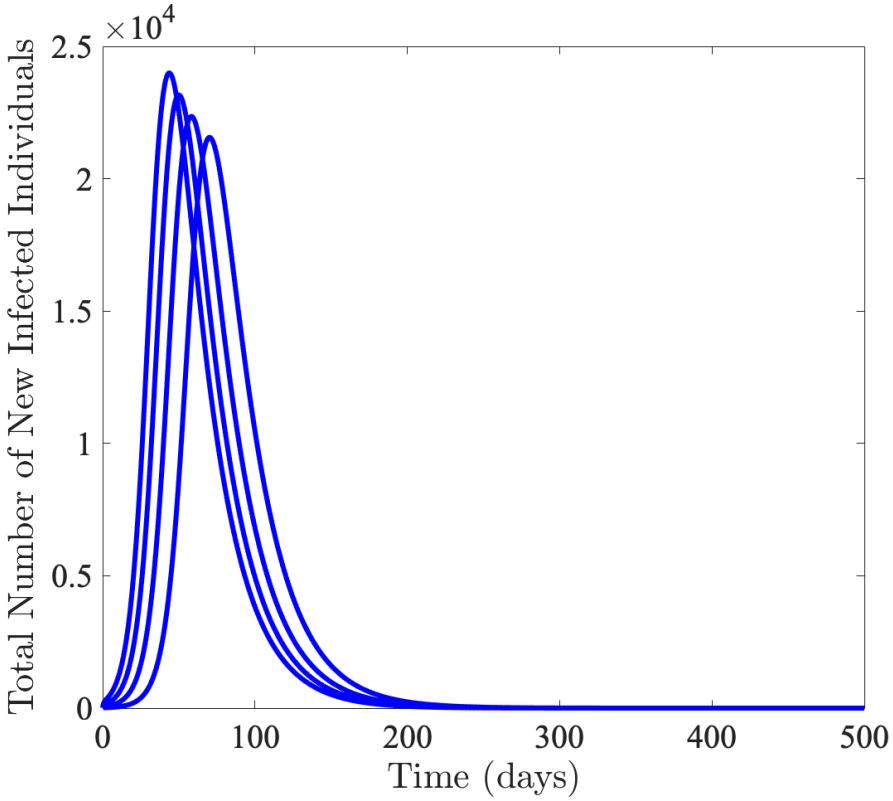

Figure 8. Simulations of the extended model (4.6), showing a time series of the total number of new cases as a function of time using the parameter values given in Table 7, with $\varepsilon_{mh} = \varepsilon_{mc} = 0.7$ and $c_{mh} = c_{mc} = 0.45$ (so that, $\widetilde{\mathbb{R}}_{CM} = 0.836 < 1$), showing convergence of all of the initial conditions to the disease-free equilibrium.

5.2. Scenario 2: The effect of vaccination of humans or camels as a sole public health intervention

In this section, the extended model (4.6) will be simulated using the baseline values of the parameters in Table 7 (unless otherwise stated) to assess the population-level impact of the vaccination

program (in both the human and camel population) implemented as the sole public health intervention in the human-camel community within the Kingdom of Saudi Arabia. In other words, in this section, the extended model (4.6) will be simulated for the scenario where masking is not implemented in the Kingdom (i.e., we set $\varepsilon_{mh} = \varepsilon_{mc} = c_{mh} = c_{mc} = 0$), and vaccination is the only intervention implemented in the community. We consider the following two cases of vaccinating humans only and vaccinating camels only.

5.2.1. Scenario 2a: The effect of vaccinating humans only

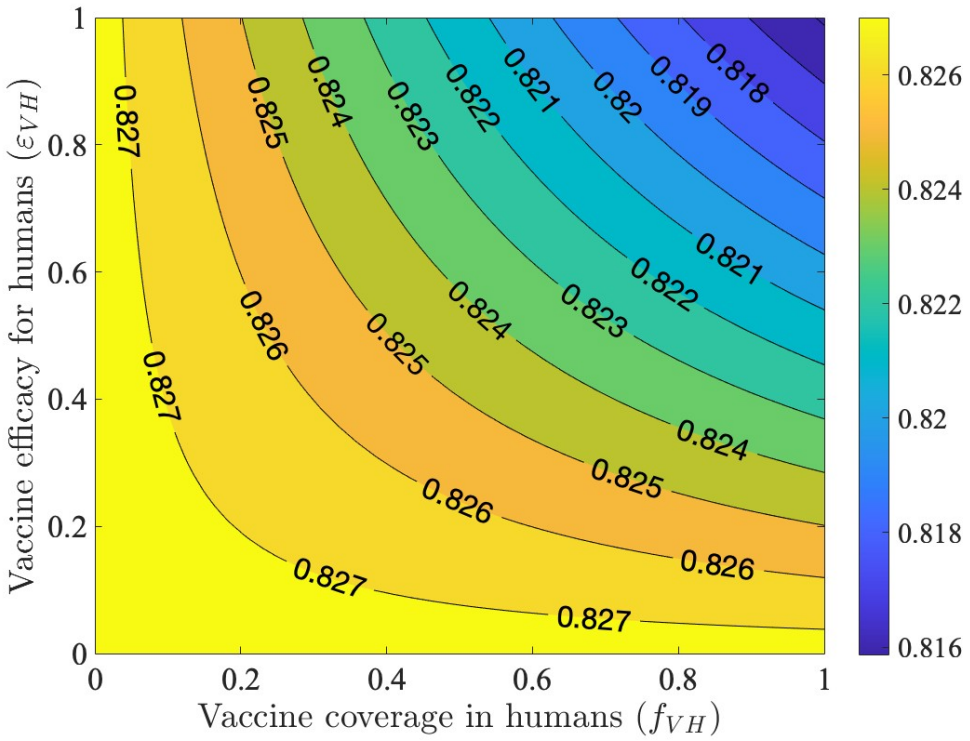

Figure 9. Simulations of the extended model (4.6) to assess the effect of vaccinating humans as a sole intervention (Scenario 2a), depicting contour plots of the human vaccination reproduction number ($\widetilde{\mathbb{R}}_{CM_H}$) of the extended model (4.6), as a function of the vaccination coverage for humans at steady-state ($f_{VH} = V_H^*/N_H^*$) and efficacy (ε_{VH}). The other parameter values used to generate these contour plots are as given in Table 7 with $\xi_{VC} = \varepsilon_{VC} = \omega_{VC} = \varepsilon_{mh} = \varepsilon_{mc} = c_{mh} = c_{mc} = 0$.

Here, the extended model (4.6) is simulated to assess the impact of vaccinating humans only (i.e., camels are not vaccinated and humans do not wear face masks). For these simulations, camels are not vaccinated (so that, $\xi_{VC} = \varepsilon_{VC} = \omega_{VC} = 0$) and humans do not wear masks in public or when in close contact with camels (i.e., $\varepsilon_{mh} = \varepsilon_{mc} = c_{mh} = c_{mc} = 0$). The results obtained are depicted by the contour plots, of the human vaccination reproduction number $\widetilde{\mathbb{R}}_{CM_H} = \mathbb{R}_{CM}|_{\xi_{VC}=\varepsilon_{VC}=\omega_{VC}=\varepsilon_{mh}=\varepsilon_{mc}=c_{mh}=c_{mc}=0}$ of the model (4.6), as a function of vaccine efficacy (ε_{VH}) and vaccine coverage in human population (f_{VH}) at the steady-state, in Figure 9. This figure shows, first of all, that, during the simulation period, the value

of the human vaccination reproduction number of the extended model, $\widetilde{\mathbb{R}}_{CM_H}$, decreases with increasing values of the vaccine efficacy and coverage in the human population. Furthermore, $\widetilde{\mathbb{R}}_{CM_H}$ lies in the range $\widetilde{\mathbb{R}}_{CM_H} \in [0.816, 0.827]$, suggesting that (since $\widetilde{\mathbb{R}}_{CM_H} < 1$) the disease can be effectively controlled (in line with Theorem 4.2) in the Kingdom. Thus, the results depicted in this figure show that even if vaccination (of humans) is not implemented in the Kingdom, the human vaccination reproduction number is below one (with the maximum value of 0.827) during the simulation period. Furthermore, this figure shows that the effect of vaccinating humans only seems to generally have a marginal impact in reducing the human vaccination reproduction number (hence, vaccinating humans seems to have only a marginal impact in reducing the disease burden in the population). For instance, using a perfect vaccine with 100% coverage could only reduce the control reproduction from the maximum value of 0.827 to 0.816 (i.e., reduction by about 10%).

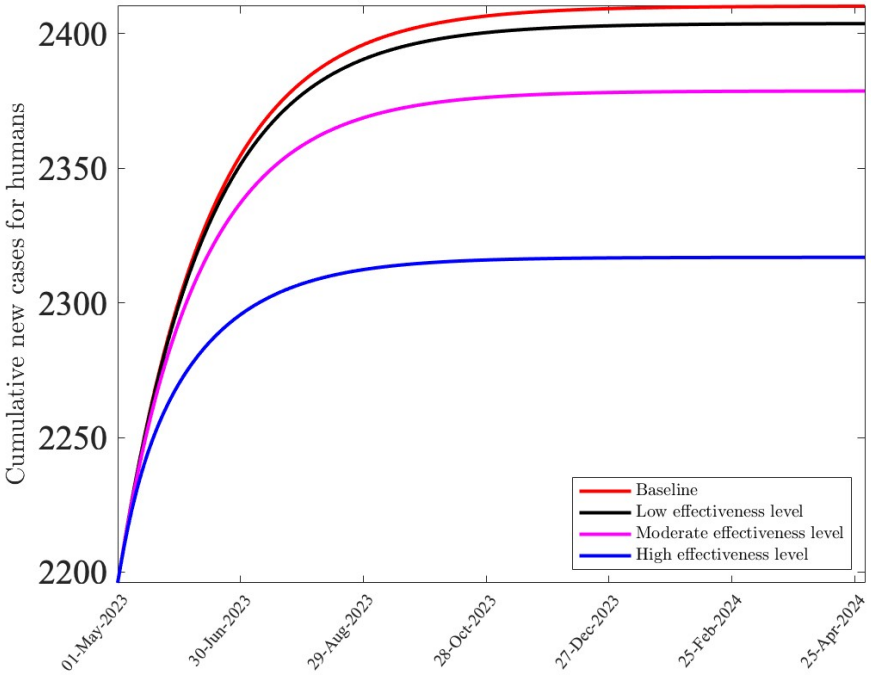

Figure 10. Simulation of the extended model (4.6) assessing the impact of vaccinating humans as a sole intervention (i.e., no vaccination of camels and no masking). Time series of the cumulative number of new MERS-CoV cases in humans, as a function of time, for various levels of effectiveness and efficacy of vaccination. Simulations are carried out for a one-year duration. (i) The red curve represents the results obtained for the case where the parameters of the model are maintained at their baseline values given in Table 7. (ii) The black curve represents the results obtained for the low effectiveness level of this intervention ($\varepsilon_{VH} = 0.25$ and $\xi_{VH} = 5 \times 10^{-3}$). (iii) The magenta curve represents the results obtained for the moderate effectiveness level of this intervention ($\varepsilon_{VH} = 0.50$ and $\xi_{VH} = 15 \times 10^{-3}$), and (iv) The blue curve represents the results obtained for the high effectiveness level of this intervention ($\varepsilon_{VH} = 0.75$ and $\xi_{VH} = 5 \times 10^{-2}$). Parameter values used in these simulations are as given in Table 7, with $\xi_{VC} = \varepsilon_{VC} = \omega_{VC} = \varepsilon_{mh} = \varepsilon_{mc} = c_{mh} = c_{mc} = 0$ and various values of ξ_{VH} and ε_{VH}.

The results for this scenario (with vaccination of humans as the only intervention implemented) is also presented in terms of the cumulative number of new cases for the following three levels of the human vaccination-only strategy:

(a) The low effectiveness level of the human vaccination-only strategy: for this strategy, we set the vaccination efficacy to be 25% (i.e., $\varepsilon_{VH} = 0.25$) and the vaccination rate to be $\xi_{VH} = 5 \times 10^{-3}$.
(b) The moderate effectiveness level of the human vaccination-only strategy: for this strategy, we set the vaccination efficacy to be 50% (i.e., $\varepsilon_{VH} = 0.50$) and the vaccination rate to be $\xi_{VH} = 15 \times 10^{-3}$.
(c) The high effectiveness level of human the vaccination-only strategy: for this strategy, we set the vaccination efficacy to be 75% (i.e., $\varepsilon_{VH} = 0.75$) and the weekly vaccination rate to be $\xi_{VH} = 5 \times 10^{-2}$.

The results obtained, depicted in Figure 10, show a marginal decrease in the cumulative number of new cases in the human population, in comparison to the baseline scenario (where all parameters are maintained at their baseline values given in Table 7). For instance, the cumulative number of new cases at the end of the one-year simulation period under the baseline scenario is 2410. This number decreases to 2403 and 2378 under the low and moderate levels of the human vaccination-only strategy, respectively (this represents less than 1% and 1.3% reduction in the cumulative new cases, in comparison to the baseline, respectively). Similarly, the cumulative number of new cases obtained using the high effectiveness level of this intervention is 2316 (which represents about 4% reduction, in comparison to the cumulative new cases generated under the baseline scenario). Thus, these simulations also confirm that, based on the parameter values used in the simulations, vaccinating humans as a sole intervention strategy would have only a marginal impact in reducing the disease burden in the Kingdom of Saudi Arabia.

5.2.2. Scenario 2b: The effect of vaccinating camels only

Here, the extended model (4.6) is simulated to assess the impact of vaccinating camels only (i.e., humans are not vaccinated and humans do not wear face masks). The simulations are also carried out for the one-year period from May 1, 2023 to April 30, 2024. Since humans are not vaccinated, we set (for these simulations) $\xi_{VH} = \varepsilon_{VH} = \omega_{VH} = 0$. Furthermore, since humans do not wear face masks under this scenario where vaccination of camels is the only intervention strategy implemented, we set the mask-related parameters to zero (i.e., we set $\varepsilon_{mh} = \varepsilon_{mc} = c_{mh} = c_{mc} = 0$). Figure 11 depicts the results obtained for this camel vaccination-only intervention scenario, showing contour plots of the camel vaccination reproduction number ($\widetilde{\mathbb{R}}_{CM_C} = \mathbb{R}_{CM}|_{\xi_{VH}=\varepsilon_{VH}=\omega_{VH}=\varepsilon_{mh}=\varepsilon_{mc}=c_{mh}=c_{mc}=0}$), as a function of the vaccine efficacy (ε_{VC}) and vaccine coverage in the camel population (f_{VC}) at the steady-state. This figure also shows a decrease in the camel vaccination reproduction number with increasing efficacy and coverage of the camel vaccine. Furthermore, the camel vaccination reproduction number lies in the range $\widetilde{\mathbb{R}}_{CM_C} \in [0.1, 0.8]$, suggesting that the disease can be effectively controlled even if the vaccination of camels (as a sole intervention) is not implemented. Unlike for the case where vaccinating humans was the sole intervention strategy implemented (which only had a marginal impact in reducing the associated reproduction number), the simulation results depicted in Figure 11 show that vaccinating camels as a sole intervention can significantly reduce the camel vaccination reproduction number (hence, reduce the disease burden in the camel population). For instance, using a camel vaccine with perfect efficacy ($\varepsilon_{VC} = 1$) and perfect coverage ($f_{VC} = 1$) reduces the maximum value of the

control reproduction number (0.8) to 0.1 (representing about 88% reduction). These results are also presented in terms of the cumulative number of new cases of MERS-CoV infection in camels, as a function of time, using the following effectiveness levels of the camel vaccination-only intervention:

(a) The low effectiveness level of the camel vaccination-only strategy: for this strategy, we set the vaccination efficacy to be 25% (i.e., $\varepsilon_{VC} = 0.25$) and the vaccination rate to be $\xi_{VC} = 2 \times 10^{-3}$.
(b) The moderate effectiveness level of the camel vaccination-only strategy: for this strategy, we set the vaccination efficacy to be 50% (i.e., $\varepsilon_{VC} = 0.50$) and the vaccination rate to be $\xi_{VC} = 6 \times 10^{-3}$.
(c) The high effectiveness level of the camel vaccination-only strategy: for this strategy, we set the vaccination efficacy to be 75% (i.e., $\varepsilon_{VC} = 0.75$) and the weekly vaccination rate to be $\xi_{VC} = 8 \times 10^{-3}$.

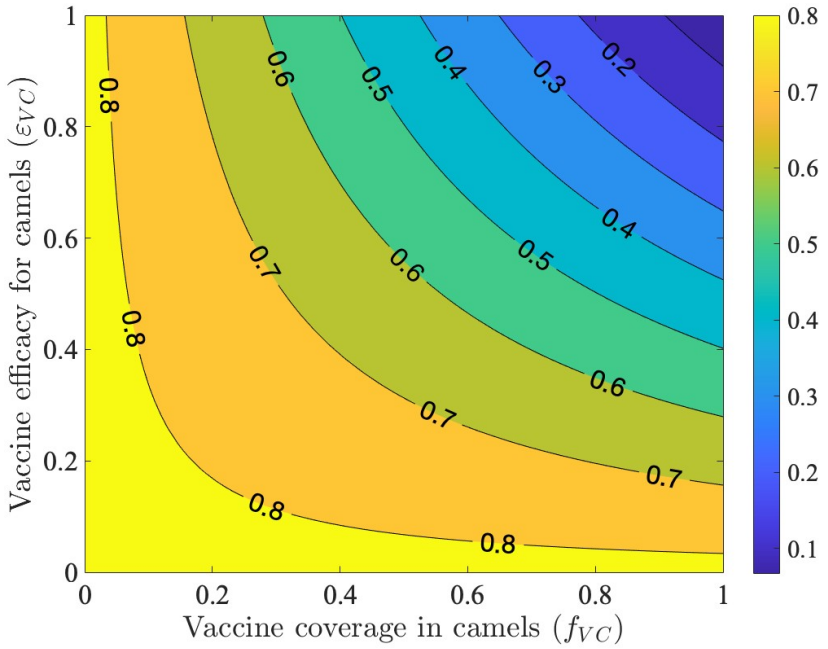

Figure 11. Simulations of the extended model (4.6) to assess the effect of vaccinating camels as a sole intervention (Scenario 2b), depicting contour plots of the camel vaccination reproduction number ($\widetilde{\mathbb{R}}_{CM_C}$) of the extended model (4.6), as a function of vaccination coverage for camels at steady-state ($f_{VC} = V_C^*/N_C^*$) and efficacy (ε_{VC}). The other parameter values used to generate the contour plots are as given in Table 7 with $\xi_{VH} = \varepsilon_{VH} = \omega_{VH} = \varepsilon_{mh} = \varepsilon_{mc} = c_{mh} = c_{mc} = 0$.

The results obtained are depicted in Figure 12, showing a significant reduction in the baseline cumulative number of new cases with an increasing effectiveness level of the camel vaccination-only intervention. For instance, the cumulative number of new cases under the baseline scenario at the end of the simulation period is 7154. It reduces to 6719 and 5413, respectively, under the low and moderate effectiveness levels of this intervention (representing, respectively, a 6% and 24% reduction, in comparison to the baseline value). Furthermore, the cumulative number of new cases recorded under the high effectiveness level of this intervention is 4730 (which represents a 34% reduction in comparison to the baseline).

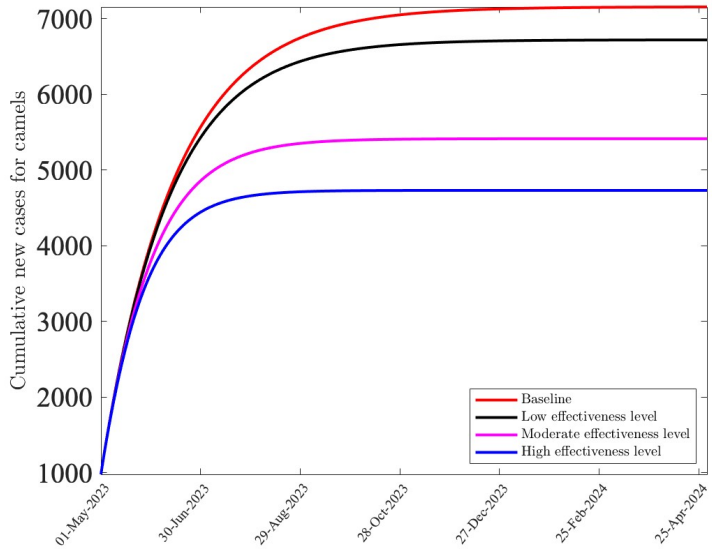

Figure 12. Simulation of the extended model (4.6) assessing the impact of vaccinating camels as a sole intervention (i.e., no vaccination of humans and no masking). Time series of the cumulative number of new MERS-CoV cases in camels, as a function of time, for various levels of effectiveness and efficacy of vaccination. Simulations are carried out for a one-year duration. (i) The red curve represents the results obtained for the case where the parameters of the model are maintained at their baseline values given in Table 7. (ii) The black curve represents the results obtained for the low effectiveness level of this intervention ($\varepsilon_{VC} = 0.25$ and $\xi_{VC} = 2 \times 10^{-3}$). (iii) The magenta curve represents the results obtained for the moderate effectiveness level of this intervention ($\varepsilon_{VC} = 0.50$ and $\xi_{VC} = 6 \times 10^{-3}$), and (iv) The blue curve represents the results obtained for the high effectiveness level of this intervention ($\varepsilon_{VC} = 0.75$ and $\xi_{VC} = 8 \times 10^{-2}$). Parameter values used in these simulations are as given in Table 7, with $\xi_{VH} = \varepsilon_{VH} = \omega_{VH} = \varepsilon_{mh} = \varepsilon_{mc} = c_{mh} = c_{mc} = 0$ and various values of ξ_{VC} and ε_{VC}.

5.3. Scenario 3: The effect of a hybrid mask-vaccination public health strategy

The extended model (4.6) will now be simulated, using the baseline values of the parameters in Table 7 (unless otherwise stated), to assess the combined population-level impacts of human and camel vaccination and mask usage interventions in the Kingdom of Saudi Arabia. This intervention is referred to as a *hybrid* strategy. The simulations for the hybrid strategy will be carried out for a one-year duration, from May 1, 2023 to April 30, 2024. Furthermore, we consider the following effectiveness levels of the hybrid vaccination and mask usage strategy:

(a) The low effectiveness level of the hybrid strategy: here, we set the protective efficacies of the vaccines (for humans and camels) and masks to be 30% (i.e., $\varepsilon_{VH} = \varepsilon_{mh} = \varepsilon_{mc} = \varepsilon_{VC} = 0.3$), mask compliance to be 25% (i.e., $c_{mh} = c_{mc} = 0.25$), and the vaccination rates for humans and camels set at $\xi_{VH} = 5 \times 10^{-3}$ and $\xi_{VC} = 2 \times 10^{-3}$, respectively.

(b) The moderate effectiveness level of the hybrid strategy: for this effectiveness level, we set the efficacies of the vaccines and mask to be 60% (i.e., $\varepsilon_{VH} = \varepsilon_{mh} = \varepsilon_{mc} = \varepsilon_{VC} = 0.6$), mask compliance

to be 50% (i.e., $c_{mh} = c_{mc} = 0.50$), and the vaccination rates for humans and camels set at $\xi_{VH} = 15 \times 10^{-3}$ and $\xi_{VC} = 6 \times 10^{-3}$, respectively.

(c) The high effectiveness level of the hybrid strategy: for the high effectiveness level of the hybrid strategy, we set the protective efficacies of the vaccines and mask to be 80% (i.e., $\varepsilon_{VH} = \varepsilon_{mh} = \varepsilon_{mc} = \varepsilon_{VC} = 0.8$), mask compliance to be 75% (i.e., $c_{mh} = c_{mc} = 0.75$), and the vaccination rates for humans and camels set, respectively, at $\xi_{VH} = 5 \times 10^{-2}$ and $\xi_{VC} = 8 \times 10^{-3}$.

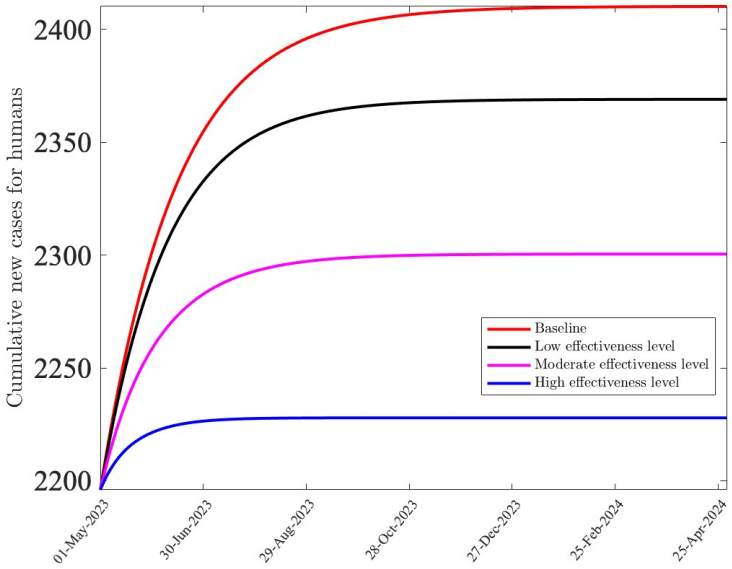

Figure 13. Simulation of the extended model (4.6) to assess the impact of the hybrid strategy (which entails the vaccination of humans and camels, and the use of face masks by humans in public and when having close contact with camels). Time series of the cumulative number of new MERS-CoV cases in humans, as a function of time, for the period from May 1, 2023 to April 30, 2024, for various effectiveness levels of the hybrid strategy. (i) The baseline strategy (red curve) where parameters are maintained at their baseline values; (ii) the low effectiveness level of the hybrid strategy (black curve); (iii) the moderate effectiveness level of the hybrid strategy (magenta curve); and (iv) the high effectiveness level of the hybrid strategy (blue curve). Parameter values used are as given in Table 7 with various values of $\xi_{VH}, \varepsilon_{VH}, \varepsilon_{mh}, \varepsilon_{mc}, c_{mh}, c_{mc}, \xi_{VC}$, and ε_{VC}.

The results obtained for a cumulative number of new cases in humans is depicted in Figure 13. This figure shows a marginal decrease in the cumulative number of new cases with increasing effectiveness levels of the hybrid strategy, in comparison to the baseline scenario. The results obtained for the cumulative number of new MERS-CoV cases in camels are depicted in Figure 14. Unlike in the case of the cumulative new cases in humans (depicted in Figure 13), this figure shows a significant decrease in the cumulative number of new MERS-CoV cases in camels with increasing effectiveness levels of the hybrid strategy, in comparison to the baseline scenario. For instance, the cumulative number of new cases at the end of the simulation period under the baseline scenario is 7154. This figure reduces to 6447 and 4902, respectively, under the low effectiveness and the moderate effectiveness level of the hybrid strategy (representing about 9% and 32% reduction, in comparison to the baseline). Similarly,

the cumulative number of new cases generated using the high effectiveness level of the hybrid strategy is 4158 (representing about 42% reduction, in comparison to the baseline value). Thus, this study shows that while the hybrid strategy only resulted in a marginal decrease in the MERS-CoV burden in humans, it resulted in a very significant reduction in the cumulative number of new cases in camels (with increasing effectiveness levels of the hybrid strategy), in comparison to the baseline scenario. In other words, the hybrid strategy will be more effective in curtailing the disease burden in camels than in the human population (*albeit* there is also an indirect benefit in reducing the burden in humans, since reducing cases in camels also implies some reduction of cases in the human population). This study suggests that strategies that focus on reducing the disease burden in the camel population (notably vaccinating camels with an effective vaccine) would significantly contribute to the effort to effectively control (or eliminate) the MERS-CoV pandemic in the human population. The extended model was simulated to illustrate the high effectiveness level of the hybrid strategy (using parameter values such that the associated reproduction number, $\widetilde{\mathbb{R}}_{CM}$, is less than one) and the results obtained, depicted in Figure 15, show convergence of all of the initial conditions to the disease-free equilibrium and disease elimination is reached within about 150 days; which is faster than the 300 days to achieve elimination predicted by simulating the model for the human vaccination-only strategy, shown in Figure 8.

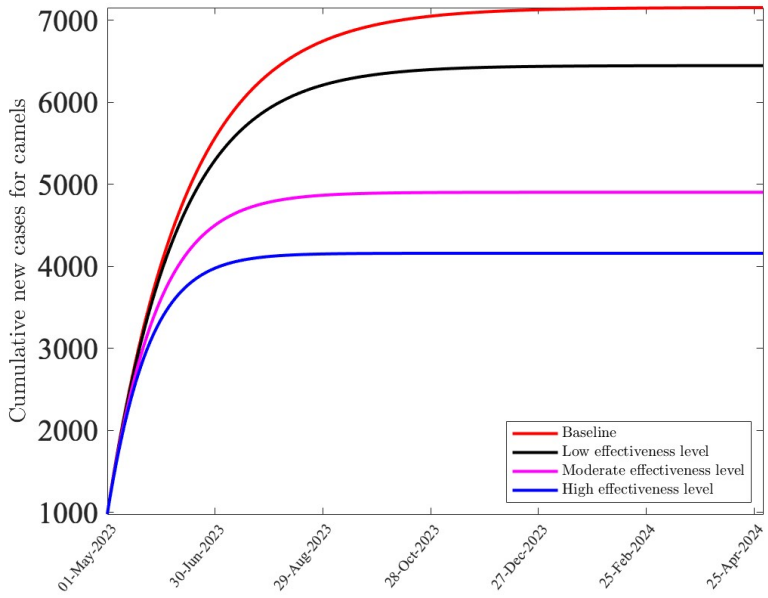

Figure 14. Simulation of the extended model (4.6) to assess the impact of the hybrid strategy (which entails the vaccination of humans and camels, and the use of face masks by humans in public and when having close contact with camels). Time series of the cumulative number of new MERS-CoV cases in camels, as a function of time, for the period from May 1, 2023 to April 30, 2024, for various effectiveness levels of the hybrid strategy. (i) The baseline strategy (red curve) where parameters are maintained at their baseline values; (ii) the low effectiveness level of the hybrid strategy (black curve); (iii) the moderate effectiveness level of the hybrid strategy (magenta curve); and (iv) the high effectiveness level of the hybrid strategy (blue curve). Parameter values used are as given in Table 7 with various values of $\xi_{VH}, \varepsilon_{VH}, \varepsilon_{mh}, \varepsilon_{mc}, c_{mh}, c_{mc}, \xi_{VC}$, and ε_{VC}.

Furthermore, it is worth stating that the cumulative number of new cases (at the end of the simulation period) for humans generated using the hybrid strategy is much lower than the corresponding cumulative number of new cases generated using any of the vaccination-only strategies discussed above. For instance, while the cumulative new cases generated using the high effectiveness level of the humans-only vaccination was about 2315 (see the blue curve in Figure 10), the cumulative number of new human cases generated using the corresponding high effectiveness level of the hybrid strategy (Figure 13, blue curve) is 2227 (which represents about 4% reduction, in comparison to the cumulative number of new cases generated using the corresponding high effectiveness level of the humans-only vaccination strategy). Similarly, the cumulative number of new cases in camels generated using the high effectiveness level of the camels-only vaccination strategy was 4700 (Figure 12, blue curve), whereas that for the corresponding high effectiveness level of the hybrid strategy is 4000 (Figure 14, blue curve), which represents about 15% reduction, in comparison to the cumulative number of new cases recorded under the camels-only vaccination strategy). The numerical simulations depicted in this section (Figures 10, 12–14) consistently highlight the fact that the intervention strategies implemented caused greater reduction in new cases in camels than in humans.

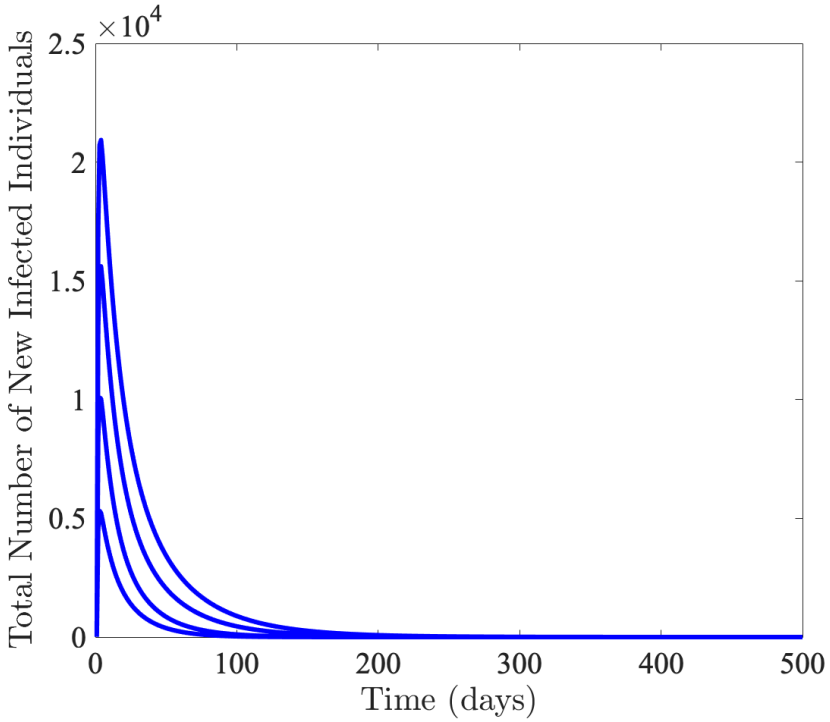

Figure 15. Simulations of the extended model (4.6), showing a time series of the total number of new cases as a function of time using the parameter values given in Table 7, with $\varepsilon_{VH} = \varepsilon_{mh} = \varepsilon_{mc} = \varepsilon_{VC} = 0.8$, $c_{mh} = c_{mc} = 0.75$, $\xi_{VH} = 5 \times 10^{-2}$, and $\xi_{VC} = 8 \times 10^{-3}$.

6. Discussion and conclusions

The Middle Eastern respiratory syndrome (MERS-CoV), a coronavirus transmitted to humans by dromedary camels, emerged out of the Kingdom of Saudi Arabia (KSA) in 2012 causing unprecedented

burden in about 30 countries (with the KSA suffering the brunt of the burden). The KSA is most vulnerable to MERS-CoV-2 outbreaks due to its hosting of several large gathering events of humans and camels, notably the annual Hajj pilgrimage (once a year) and Umrah year [8], and the camel festival in the capital city of Riyadh (which typically runs for a two-month period) [9, 10]. This study presented a new mathematical model for the transmission dynamics of MERS-CoV in the KSA. The basic model, which takes the form of a deterministic system of nonlinear differential equations, was, first of all, fitted using observed MERS-CoV data for the KSA (for the period from Week 13 to Week 42 of 2013), and the fitted model was used to estimate the unknown parameters of the model. The data for Week 43 of 2013 to Week 9 of 2014 was used to cross-validate the model (4.6). This cross-validation, together with simulations involving the cumulative cases of MERS-CoV, presented a good match to the observed data in the Kingdom of Saudi Arabia.

The basic model was rigorously analyzed to gain insight into its qualitative properties. Specifically, results with respect to the boundedness and invariance of its solutions, as well as the asymptotic stability properties of its associated disease-free equilibrium, were provided. Specifically, it was shown that the disease-free equilibrium of the model was locally asymptotically stable whenever its reproduction number (denoted by $\mathbb{R}_{0M}$) was less than unity. The epidemiological implication of this result is that the effective control of the disease in the human-camel population within the KSA (when $\mathbb{R}_{0M}$) depends on the initial sizes of the sub-populations of the model (in other words, disease control or elimination depends on whether or not the initial number of infected humans and camels lie within the basin of attraction of the disease-free equilibrium). Using the fixed and estimated parameters of the basic model, this study showed that the value of $\mathbb{R}_{0M}$ for the Kingdom of Saudi Arabia was approximately 0.84, suggesting that the prospects for MERS-CoV elimination in the KSA are highly promising.

Global sensitivity analysis was carried out, using Latin hypercube sampling and partial rank correlation coefficients (PRCCs), to determine the parameters of the model (2.1) that have the greatest influence on the value of the chosen response function ($\mathbb{R}_{0M}$, which is a measure of the burden of the disease in the Kingdom). The top five PRCC-ranked parameters identified in this study were: (a) the parameters for the rates of camels recovered from the MERS-CoV infection (γ_C), (b) the transmission rate from infected to susceptible camels (β_{CC}), and (c) the transmission rate from infected humans to susceptible camels (β_{HC}). The numerical size and (negative) sign of the computed PRCC values of the parameters of the model (4.6) (tabulated in Table 4) indicate that reduction of the infection rate of infectious camels to susceptible camels (β_{CC}) and the infection rate from infectious humans to susceptible camels (β_{HC}), which can be achieved, for instance, by the quarantine and isolation of suspected and symptomatic humans and camels, will lead to a corresponding reduction of $\mathbb{R}_{0M}$ (hence, a reduction in disease burden). The use of effective face masks by humans in the public or when having contact with camels, social-distancing between humans, and community lockdowns in both populations will also decrease the transmission rate parameters (hence, decrease the response function, $\mathbb{R}_{0M}$; and, consequently, the disease burden in both host populations). Similarly, the PRCC values obtained (tabulated in Table 4) show that the implementation of control and mitigation measures that increase the value of the recovery rate parameter for camels (γ_C), such as by the isolation and treatment of infectious camels with highly effective antiviral drugs, will correspondingly reduce the response function (and, consequently, reduce the burden of the disease in the Kingdom).

The basic model was extended to incorporate non-pharmaceutical and pharmaceutical public health interventions, notably the use of face masks by humans in public and when having close contact with

camels, and vaccination of both humans and camels. Here, too, the disease-free equilibrium of the resulting extended model (4.6) was shown to be locally asymptotically stable whenever its associated control reproduction number (denoted by $\mathbb{R}_{CM}$) was less than one. The implication of this result is that the implementation of the aforementioned public health interventions could lead to the effective control (or elimination) of MERS-CoV in the Kingdom of Saudi Arabia if the interventions could bring (and maintain) the value of the control reproduction number ($\mathbb{R}_{CM}$) to be below one (provided the initial number of infected individuals and camels lie within the basin of attraction of the DFE).

The extended model was then simulated to assess the population-level impact of the chosen public health interventions. Specifically, simulations were, first, carried out (for a period of one year) to assess the impact of face mask use as a sole intervention (where the masks are worn by humans when they come in close proximity with camels only) on the transmission dynamics and control of MERS-CoV in the KSA. The extended model was simulated for the special case without vaccination and humans do not wear face masks in public. The simulation results showed that the associated control reproduction number $\widetilde{\mathbb{R}}_{CM_{mc}}$ decreased with increasing values of the mask efficacy and compliance, and that $\widetilde{\mathbb{R}}_{CM_{mc}}$ lied in the range $\widetilde{\mathbb{R}}_{CM_{mc}} \in [0.85, 1.1]$ (suggesting that the use of face masks as a sole intervention can lead to the elimination of the disease in the population, depending on the efficacy of, and compliance in, mask usage in the community. For example, this figure shows that if surgical masks (with an estimated efficacy of about 70%) is prioritized, the disease can be effectively controlled or eliminated (in both the human and camel populations) if at least 45% of the human population consistently wear such masks whenever they are within close proximity to camels. Then, we studied the effects of vaccination of humans as a sole intervention strategy implemented in the Kingdom (i.e., humans do not wear face masks in public or when having close contact with camels, and camels are not vaccinated) under three effectiveness levels of this human vaccination-only strategy (namely, low, moderate, and high). The results obtained, for the case where only humans are vaccinated, showed that although the the burden of MERS-CoV in the human population decreases with an increasing effectiveness level of this (human vaccination-only) intervention (as measured in terms of the reduction in the associated control reproduction number of the extended model or the cumulative number of new cases and cumulative mortality in humans), in comparison to the baseline scenario, this reduction was quite marginal. In other words, these simulations showed that, based on the parameter values in the simulations, vaccinating humans (as a sole intervention) will only offer a marginal impact in reducing the burden of the MERS-CoV pandemic in the Kingdom of Saudi Arabia. On the other hand, the simulations for the case where vaccination of camels was the sole intervention implemented (and humans are not vaccinated and do not wear masks) showed, over the same one-year period, a significant reduction in both the associated reproduction number and the cumulative number of new MERS-COV cases in camels with an increasing effectiveness level of this (camels vaccination only) intervention strategy, in comparison to the baseline scenario. For instance, these simulations show that while the moderate effectiveness level of this strategy could reduce the baseline cumulative new cases at the end of the one-year simulation period by about 24%, the high effectiveness level of this intervention reduces the cumulative number of new cases by about 34%.

Finally, the extended model was used to simulate the population-level impact of a *hybrid* strategy, where both humans and camels are vaccinated and humans wear mask in public and when having close contact with camels. Here, too, three effectiveness levels (low, moderate, and high) of the hybrid strategy were considered. The simulation results obtained showed that while this strategy only offers

a marginal decrease in the disease burden in humans, with an increasing effectiveness level, in comparison to the baseline, it resulted in a marked decrease in the cumulative number of new MERS-CoV cases in camels (for instance, the moderate and high effectiveness levels of this intervention reduced the baseline cumulative new cases in camels by 32% and 42%, respectively). Thus, this study shows that, while the hybrid strategy only offers a marginal reduction in the burden of the MERS-CoV pandemic in humans, it can result in a significant reduction in the cumulative new cases in camels. The cumulative number of new cases for humans (camels) generated using the hybrid strategy was consistently lower than the cumulative number of new cases obtained using a vaccination-only strategy for humans (camels). For instance, the simulations in this study showed that the high effectiveness level of the hybrid strategy reduced the cumulative number of new cases in humans (camels) by about 4% (15%), in comparison to the corresponding cumulative new cases generated using a vaccination-only strategy (and more of such reductions were recorded in camels than in humans). Thus, this study emphasizes control measures that focus on the camel population (e.g., routine vaccination of camels using an effective vaccine with moderate to high coverage), instead of those that focus on humans. In summary, the analytical and simulation results generated in this study showed that the prospects for the effective control of MERS-CoV in the Kingdom of Saudi Arabia are promising using the public health interventions described in the study, provided their effectiveness levels are high enough. In particular, the implementation of a hybrid strategy that entails the vaccination of both humans and camels and the use of face masks by humans in public and when having close contact with camels can significantly reduce the disease burden in the Kingdom of Saudi Arabia. Greater reductions (in the burden of the disease) were recorded in the camel population than in the human population (the impacts of the interventions in reducing the burden of the pandemic in the latter, from the baseline scenario, were consistently quite marginal). Thus, this study showed that efforts should be focused on prioritizing interventions that effectively control the disease in the camel population, rather than in the human population. In other words, this study suggests that control resources should be prioritized to disease control in camels rather than humans.

Use of AI tools declaration

The authors declare they have not used Artificial Intelligence (AI) tools in the creation of this article.

Acknowledgments

ABG acknowledges the support, in part, of the National Science Foundation (DMS-2052363). AA acknowledges the scholarship received from the University of Tabuk, Saudi Arabia. The authors are grateful to the three anonymous reviewers for their very constructive comments.

Conflict of interest

Abba B. Gumel is an editorial board member for Mathematical Biosciences and Engineering and was not involved in the editorial review or the decision to publish this article. All authors declare that there are no competing interests.

References

1. A. M. Zaki, S. Van Boheemen, T. M. Bestebroer, A. D. M. E. Osterhaus, R. A. M. Fouchier, Isolation of a novel coronavirus from a man with pneumonia in Saudi Arabia, *N. Engl. J. Med.*, **367** (2012), 1814–1820. https://doi.org/10.1056/NEJMoa1211721
2. T. M. Malik, A. A. Alsaleh, A. B. Gumel, M. A. Safi, Optimal strategies for controlling the MERS coronavirus during a mass gathering, *Global J. Pure Appl. Math.*, **11** (2015), 4831–4865.
3. J. A. Tawfiq, C. A. H. Smallwood, K. G. Arbuthnott, M. S. K. Malik, M. Barbeschi, Z. A. Memish, Emerging respiratory and novel coronavirus 2012 infections and mass gatherings, *EMHJ-East. Mediterr. Health J.*, **19** (2013), S48–S54. https://doi.org/10.26719/2013.19.supp1.S48
4. A. Alatawi, *Mathematical Assessment of the Transmission Dynamics and Control of MERS-CoV and SARS-CoV-2 in the Kingdom of Saudi Arabia*, PhD thesis, Arizona State University, 2023.
5. J. Min, E. Cella, M. Ciccozzi, A. Pelosi, M. Salemi, M. Prosperi, The global spread of middle east respiratory syndrome: an analysis fusing traditional epidemiological tracing and molecular phylodynamics, *Global Health Res. Policy*, **1** (2016), 1–14. https://doi.org/10.1186/s41256-016-0014-7
6. K. P. Devakumar, *MERS Outbreaks Data 2012–2019*, Available from: https://www.kaggle.com/datasets/imdevskp/mers-outbreak-dataset-20122019.
7. World Health Organization, *Middle East Respiratory Syndrome: Global Summary and Assessment of Risk*, 2022. Available from: https://iris.who.int/bitstream/handle/10665/364525/WHO-MERS-RA-2022.1-eng.pdf.
8. ARAB NEWS, *Saudi Arabia: Hajj 2020 to Be Held with Limited Number of Pilgrims*, 2023. Available from: https://www.arabnews.com/node/1693856/saudi-arabia.
9. S. Gazette, *International Camel Conference to be Held to Utilize Products, Stimulate Investment*, 2021. Available from: https://saudigazette.com.sa/article/610500.
10. AlARABIYA news, *Camel Club*, 2023. Available from: https://english.alarabiya.net/views/2024/05/02/camel-racing-an-enduring-staple-of-arabian-gulf-sports-scene-now-and-in-the-future.
11. F. A. Rabi, M. S. A. Zoubi, G. A. Kasasbeh, D. M. Salameh, A. D. A. Nasser, SARS-CoV-2 and coronavirus disease 2019: what we know so far, *Pathogens*, **9** (2020), 231. https://doi.org/10.3390/pathogens9030231
12. A. B. Gumel, E. A. Iboi, C. N. Ngonghala, E. H. Elbasha, A primer on using mathematics to understand COVID-19 dynamics: Modeling, analysis and simulations, *Infect. Dis. Modell.*, **6** (2021), 148–168. https://doi.org/10.1016/j.idm.2020.11.005
13. W. Li, Z. Shi, M. Yu, W. Ren, C. Smith, J. H. Epstein, et al., Bats are natural reservoirs of SARS-like coronaviruses, *Science*, **310** (2005), 676–679. https://doi.org/10.1126/science.1118391
14. N. L. Ithete, S. Stoffberg, V. M. Corman, V. M. Cottontail, L. R. Richards, M. C. Schoeman, et al., Close relative of human middle east respiratory syndrome coronavirus in bat, South Africa, *Emerging Infect. Dis.*, **19** (2013), 1697. https://doi.org/10.3201/eid1910.130946

15. G. Chowell, S. Blumberg, L. Simonsen, M. A. Miller, C. Viboud, Synthesizing data and models for the spread of MERS-CoV, 2013: key role of index cases and hospital transmission, *Epidemics*, **9** (2014), 40–51. https://doi.org/10.1016/j.epidem.2014.09.011

16. T. A. Aljasim, A. Almasoud, H. A. Aljami, M. W. Alenazi, S. A. Alsagaby, A. N. Alsaleh, et al., High rate of circulating MERS-CoV in dromedary camels at slaughterhouses in Riyadh, 2019, *Viruses*, **12** (2020), 1215. https://doi.org/10.3390/v12111215

17. M. E. Killerby, H. M. Biggs, C. M. Midgley, S. I. Gerber, J. T. Watson, Middle east respiratory syndrome coronavirus transmission, *Emerging Infect. Dis.*, **26** (2020), 191. https://doi.org/10.3201/eid2602.190697

18. M. G. Hemida, A. Alnaeem, Some one health based control strategies for the middle east respiratory syndrome coronavirus, *One Health*, **8** (2019), 100102. https://doi.org/10.1016/j.onehlt.2019.100102

19. A. S. Omrani, J. A. Al-Tawfiq, Z. A. Memish, Middle east respiratory syndrome coronavirus (MERS-CoV): animal to human interaction, *Pathog. Global Health*, **109** (2015), 354–362. https://doi.org/10.1080/20477724.2015.1122852

20. Nature, *Did Pangolins Spread the China Coronavirus to People*, 2023. Available from: https://www.nature.com/articles/d41586-020-00364-2.

21. M. G. Hemida, R. A. Perera, P. Wang, M. A. Alhammadi, L. Y. Siu, M. Li, et al., Middle east respiratory syndrome (MERS) coronavirus seroprevalence in domestic livestock in Saudi Arabia, 2010 to 2013, *Eurosurveillance*, **18** (2013), 20659. https://doi.org/10.2807/1560-7917.ES2013.18.50.20659

22. A. Mostafa, A. Kandeil, M. Shehata, R. E. Shesheny, A. M. Samy, G. Kayali, et al., Middle east respiratory syndrome coronavirus (MERS-CoV): State of the science, *Microorganisms*, **8** (2020), 991. https://doi.org/10.3390/microorganisms8070991

23. N. Van Doremalen, T. Bushmaker, V. J. Munster, Stability of middle east respiratory syndrome coronavirus (MERS-CoV) under different environmental conditions, *Eurosurveillance*, **18** (2013), 20590. https://doi.org/10.2807/1560-7917.ES2013.18.38.20590

24. M. G. Hemida, A. Al-Naeem, R. A. P. M. Perera, A. W. H. Chin, L. L. M. Poon, M. Peiris, Lack of middle east respiratory syndrome coronavirus transmission from infected camels, *Emerging Infect. Dis.*, **21** (2015), 699. https://doi.org/10.3201/eid2104.141949

25. R. Conzade, R. Grant, M. R. Malik, A. Elkholy, M. Elhakim, D. Samhouri, et al., Reported direct and indirect contact with dromedary camels among laboratory-confirmed MERS-CoV cases, *Viruses*, **10** (2018), 425. https://doi.org/10.3390/v10080425

26. D. R. Adney, N. van Doremalen, V. R. Brown, T. Bushmaker, D. Scott, E. de Wit, et al., Replication and shedding of MERS-CoV in upper respiratory tract of inoculated dromedary camels, *Emerging Infect. Dis.*, **20** (2014), 1999. https://doi.org/10.3201/eid2012.141280

27. D. R. Adney, L. Wang, N. Van Doremalen, W. Shi, Y. Zhang, W. Kong, et al., Efficacy of an adjuvanted middle east respiratory syndrome coronavirus spike protein vaccine in dromedary camels and alpacas, *Viruses*, **11** (2019), 212. https://doi.org/10.3390/v11030212

28. I. Ghosh, S. K. S. Nadim, J. Chattopadhyay, Zoonotic MERS-CoV transmission: modeling, backward bifurcation and optimal control analysis, *Nonlinear Dyn.*, **103** (2021), 2973–2992. https://doi.org/10.1007/s11071-021-06266-w

29. J. A. Al-Tawfiq, Z. A. Memish, Middle east respiratory syndrome coronavirus: epidemiology and disease control measures, *Infect. Drug Resist.*, **7** (2014), 281. https://doi.org/10.2147/IDR.S51283

30. D. S. Hui, E. I. Azhar, Y. J. Kim, Z. A. Memish, M. Oh, A. Zumla, Middle east respiratory syndrome coronavirus: risk factors and determinants of primary, household, and nosocomial transmission, *Lancet Infect. Dis.*, **18** (2018), e217–e227. https://doi.org/10.1016/S1473-3099(18)30127-0

31. M. Tahir, S. I. A. Shah, G. Zaman, T. Khan, A dynamic compartmental mathematical model describing the transmissibility of MERS-CoV virus in public, *Punjab Univ. J. Math.*, **51** (2020).

32. Z. A. Memish, A. I. Zumla, A. Assiri, Middle east respiratory syndrome coronavirus infections in health care workers, *N. Engl. J. Med.*, **369** (2013), 884–886. https://doi.org/10.1056/NEJMc1308698

33. A. R. Zhang, W. Q. Shi, K. Liu, X. L. Li, M. J. Liu, W. H. Zhang, et al., Epidemiology and evolution of middle east respiratory syndrome coronavirus, 2012–2020, *Infect. Dis. Poverty*, **10** (2021), 1–13.

34. Z. Wu, D. Harrich, Z. Li, D. Hu, D. Li, The unique features of SARS-CoV-2 transmission: Comparison with SARS-CoV, MERS-CoV and 2009 H1N1 pandemic influenza virus, *Rev. Med. Virol.*, **31** (2021), e2171. https://doi.org/10.1002/rmv.2171

35. N. C. Peeri, N. Shrestha, M. S. Rahman, R. Zaki, Z. Tan, S. Bibi, et al., The SARS, MERS and novel coronavirus (COVID-19) epidemics, the newest and biggest global health threats: what lessons have we learned, *Int. J. Epidemiol.*, **49** (2020), 717–726.

36. V. C. C. Cheng, K. K. W. To, H. Tse, I. F. N. Hung, K. Y. Yuen, Two years after pandemic influenza a/2009/H1N1: what have we learned, *Clin. Microbiol. Rev.*, **25** (2012), 223–263. https://doi.org/10.1128/CMR.05012-11

37. E. A. Nardell, R. R. Nathavitharana, Airborne spread of SARS-CoV-2 and a potential role for air disinfection, *JAMA*, **324** (2020), 141–142. https://doi.org/10.1001/jama.2020.7603

38. S. Safdar, A. B. Gumel, Mathematical assessment of the role of interventions against SARS-CoV-2, in *Mathematics of Public Health: Mathematical Modelling from the Next Generation*, (2023), 243–294. https://doi.org/10.1007/978-3-031-40805-2_10

39. B. Ganesh, T. Rajakumar, M. Manikandan, J. Nagaraj, A. Santhakumar, A. Elangovan, et al., Epidemiology and pathobiology of SARS-CoV-2 (COVID-19) in comparison with SARS, MERS: An updated overview of current knowledge and future perspectives, *Clin. Epidemiol. Global Health*, **10** (2021), 100694.

40. A. Zumla, D. S. Hui, S. Perlman, Middle east respiratory syndrome, *Lancet*, **386** (2015), 995–1007. https://doi.org/10.1016/S0140-6736(15)60454-8

41. E. I. Azhar, S. A. El-Kafrawy, S. A. Farraj, A. M. Hassan, M. S. Al-Saeed, A. M. Hashem, et al., Evidence for camel-to-human transmission of MERS coronavirus, *N. Engl. J. Med.*, **370** (2014), 2499–2505. https://doi.org/10.1056/NEJMoa1401505

42. J. S. Chung, M. L. Ling, W. H. Seto, B. S. P. Ang, P. A. Tambyah, Debate on MERS-CoV respiratory precautions: surgical mask or N95 respirators, *Singapore Med. J.*, **55** (2014), 294. https://doi.org/10.11622/smedj.2014076

43. A. M. Patil, J. R. Göthert, V. Khairnar, Emergence, transmission, and potential therapeutic targets for the COVID-19 pandemic associated with the SARS-CoV-2, *Cell Physiol. Biochem.*, **54** (2020), 767–790. https://doi.org/10.33594/000000254

44. H. H. Balkhy, T. H. Alenazi, M. M. Alshamrani, H. Baffoe-Bonnie, Y. Arabi, R. Hijazi, et al., Description of a hospital outbreak of middle east respiratory syndrome in a large tertiary care hospital in Saudi Arabia, *Infect. Control Hosp. Epidemiol.*, **37** (2016), 1147–1155. https://doi.org/10.1017/ice.2016.132

45. I. K. Oboho, S. M. Tomczyk, A. M. Al-Asmari, A. A. Banjar, H. Al-Mugti, M. S. Aloraini, et al., 2014 MERS-CoV outbreak in jeddah—a link to health care facilities, *N. Engl. J. Med.*, **372** (2015), 846–854. https://doi.org/10.1056/NEJMoa1408636

46. J. Liu, W. Xie, Y. Wang, Y. Xiong, S. Chen, J. Han, et al., A comparative overview of COVID-19, MERS and SARS, *Int. J. Surg.*, **81** (2020), 1–8. https://doi.org/10.1016/j.ijsu.2020.07.032

47. N. K. Alharbi, O. H. Ibrahim, A. Alhafufi, S. Kasem, A. Aldowerij, R. Albrahim, et al., Challenge infection model for mers-cov based on naturally infected camels, *Virol. J.*, **17** (2020), 1–7. https://doi.org/10.1186/s12985-020-01347-5

48. S. S. Sohrab, S. A. El-Kafrawy, Z. Mirza, A. M. Hassan, F. Alsaqaf, E. I. Azhar, Computational design and experimental evaluation of MERS-CoV sirnas in selected cell lines, *Diagnostics*, **13** (2023), 151. https://doi.org/10.3390/diagnostics13010151

49. N. K. Alharbi, F. Aljamaan, H. A. Aljami, M. W. Alenazi, H. Albalawi, A. Almasoud, et al., Immunogenicity of high-dose MAV-based MERS vaccine candidate in mice and camels, *Vaccines*, **10** (2022), 1330. https://doi.org/10.3390/vaccines10081330

50. Y. Zhou, S. Jiang, L. Du, Prospects for a MERS-CoV spike vaccine, *Expert Rev. Vaccines*, **17** (2018), 677–686. https://doi.org/10.1080/14760584.2018.1506702

51. B. L. Haagmans, J. M. A. Van Den Brand, V. S. Raj, A. Volz, P. Wohlsein, S. L. Smits, et al., An orthopoxvirus-based vaccine reduces virus excretion after MERS-CoV infection in dromedary camels, *Science*, **351** (2016), 77–81. https://doi.org/10.1126/science.aad1283

52. M. Kandeel, A. I. Al-Mubarak, Camel viral diseases: Current diagnostic, therapeutic, and preventive strategies, *Front. Vet. Sci.*, **9** (2022), 915475. https://doi.org/10.3389/fvets.2022.915475

53. N. K. Alharbi, Vaccines against middle east respiratory syndrome coronavirus for humans and camels, *Rev. Med. Virol.*, **27** (2017), e1917. https://doi.org/10.1002/rmv.1917

54. Inc. INOVIO Pharmaceuticals, *Inovio Doses First Participant in Phase 2 Trial for Its DNA Vaccine Against Middle East Respiratory Syndrome (MERS), A Coronavirus Disease*, 2023. Available from: https://ir.inovio.com/news-releases/news-releases-details/2021/INOVIO-Doses-First-Participant-in-Phase-2-Trial-for-its-DNA-Vaccine-Against-Middle-East-Respiratory-Syndrome-MERS-a-Coronavirus-Disease/default.aspx.

55. I. M. Mackay, K. E. Arden, MERS coronavirus: diagnostics, epidemiology and transmission, *Virol. J.*, **12** (2015), 1–21. https://doi.org/10.1186/s12985-015-0439-5

56. Inc. Johnson & Johnson Services, *Johnson & Johnson Announces New Collaboration to Advance Novel Vaccine for MERS*, 2023. Available from: https://www.jnj.com/media-center/press-releases/johnson-johnson-announces-new-collaboration-to-advance-novel-vaccine-for-mers.

57. G. M. Warimwe, J. Gesharisha, B. V. Carr, S. Otieno, K. Otingah, D. Wright, et al., Chimpanzee adenovirus vaccine provides multispecies protection against rift valley fever, *Sci. Rep.*, **6** (2016), 1–7. https://doi.org/10.1038/srep20617

58. T. Sardar, I. Ghosh, X. Rodó, J. Chattopadhyay, A realistic two-strain model for MERS-CoV infection uncovers the high risk for epidemic propagation, *PLoS Negl.Trop. Dis.*, **14** (2020), e0008065. https://doi.org/10.1371/journal.pntd.0008065

59. T. Oraby, M. G. Tyshenko, H. H. Balkhy, Y. Tasnif, A. Quiroz-Gaspar, Z. Mohamed, et al., Analysis of the healthcare MERS-CoV outbreak in king abdulaziz medical center, Riyadh, Saudi Arabia, June–August 2015 using a SEIR ward transmission model, *Int. J. Environ. Res. Public Health*, **17** (2020), 2936. https://doi.org/10.3390/ijerph17082936

60. S. Cauchemez, P. Nouvellet, A. Cori, T. Jombart, T. Garske, H. Clapham, et al., Unraveling the drivers of MERS-CoV transmission, *Proc. Natl. Acad. Sci.*, **113** (2016), 9081–9086. https://doi.org/10.1073/pnas.1519235113

61. M. John, H. Shaiba, Main factors influencing recovery in MERS CoV patients using machine learning, *J. Infect. Public Health*, **12** (2019), 700–704. https://doi.org/10.1016/j.jiph.2019.03.020

62. S. Hussain, O. Tunç, G. ur Rahman, H. Khan, E. Nadia, Mathematical analysis of stochastic epidemic model of MERS-corona & application of ergodic theory, *Math. Comput. Simul.*, **207** (2023), 130–150. https://doi.org/10.1016/j.matcom.2022.12.023

63. Q. Lin, A. P. Y. Chiu, S. Zhao, D. He, Modeling the spread of middle east respiratory syndrome coronavirus in Saudi Arabia, *Stat. Methods Med. Res.*, **27** (2018), 1968–1978. https://doi.org/10.1177/0962280217746442

64. C. Poletto, V. Colizza, P. Y. Boëlle, Quantifying spatiotemporal heterogeneity of MERS-CoV transmission in the middle east region: A combined modelling approach, *Epidemics*, **15** (2016), 1–9. https://doi.org/10.1016/j.epidem.2015.12.001

65. B. Fatima, M. A. Alqudah, G. Zaman, F. Jarad, T. Abdeljawad, Modeling the transmission dynamics of middle eastern respiratory syndrome coronavirus with the impact of media coverage, *Results Phys.*, **24** (2021), 104053. https://doi.org/10.1016/j.rinp.2021.104053

66. J. Rui, Q. Wang, J. Lv, B. Zhao, Q. Hu, H. Du, et al., The transmission dynamics of middle east respiratory syndrome coronavirus, *Travel Med. Infect. Dis.*, **45** (2022), 102243. https://doi.org/10.1016/j.tmaid.2021.102243

67. J. Lee, G. Chowell, E. Jung, A dynamic compartmental model for the middle east respiratory syndrome outbreak in the republic of Korea: a retrospective analysis on control interventions and superspreading events, *J. Theor. Biol.*, **408** (2016), 118–126. https://doi.org/10.1016/j.jtbi.2016.08.009

68. W. Jansen, V. Lakshmikantham, S. Leela, A. A. Martynyuk, *Stability Analysis of Nonlinear Systems*, Marcel Dekker inc., 1995.

69. A. B. Gumel, C. C. McCluskey, P. van den Driessche, Mathematical study of a staged-progression HIV model with imperfect vaccine, *Bull. Math. Biol.*, **68** (2006), 2105–2128. https://doi.org/10.1007/s11538-006-9095-7

70. J. Mohammed-Awel, E. A. Iboi, A. B. Gumel, Insecticide resistance and malaria control: A genetics-epidemiology modeling approach, *Math. Biosci.*, **325** (2020), 108368. https://doi.org/10.1016/j.mbs.2020.108368

71. S. M. Garba, J. M. S. Lubuma, B. Tsanou, Modeling the transmission dynamics of the COVID-19 pandemic in South Africa, *Math. Biosci.*, **328** (2020), 108441. https://doi.org/10.1016/j.mbs.2020.108441

72. H. R. Thieme, *Mathematics in Population Biology*, Princeton University Press, 2018.

73. P. Van den Driessche, J. Watmough, Reproduction numbers and sub-threshold endemic equilibria for compartmental models of disease transmission, *Math. Biosci.*, **180** (2002), 29–48. https://doi.org/10.1016/S0025-5564(02)00108-6

74. O. Diekmann, J. A. P. Heesterbeek, J. A. J. Metz, On the definition and the computation of the basic reproduction ratio R_0 in models for infectious diseases in heterogeneous populations, *J. Math. Biol.*, **28** (1990), 365–382. https://doi.org/10.1007/BF00178324

75. K. O. Okuneye, J. X. Velasco-Hernandez, A. B. Gumel, The "unholy" chikungunya–dengue–Zika trinity: a theoretical analysis, *J. Biol. Syst.*, **25** (2017), 545–585. https://doi.org/10.1142/S0218339017400046

76. H. T. Banks, M. Davidian, J. R. Samuels, K. L. Sutton, An inverse problem statistical methodology summary, in *Mathematical and Statistical Estimation Approaches in Epidemiology*, (2009), 249–302. https://doi.org/10.1007/978-90-481-2313-1

77. G. Chowell, Fitting dynamic models to epidemic outbreaks with quantified uncertainty: A primer for parameter uncertainty, identifiability, and forecasts, *Infect. Dis. Modell.*, **2** (2017), 379–398. https://doi.org/10.1016/j.idm.2017.08.001

78. C. N. Ngonghala, E. Iboi, S. Eikenberry, M. Scotch, C. R. MacIntyre, M. H. Bonds, et al., Mathematical assessment of the impact of non-pharmaceutical interventions on curtailing the 2019 novel coronavirus, *Math. Biosci.*, **325** (2020), 108364. https://doi.org/10.1016/j.mbs.2020.108364

79. S. M. Blower, H. Dowlatabadi, Sensitivity and uncertainty analysis of complex models of disease transmission: an HIV model, as an example, *Int. Stat. Rev.*, **62** (1994), 229–243. https://doi.org/10.2307/1403510

80. S. Marino, I. B. Hogue, C. J. Ray, D. E. Kirschner, A methodology for performing global uncertainty and sensitivity analysis in systems biology, *J. Theor. Biol.*, **254** (2008), 178–196. https://doi.org/10.1016/j.jtbi.2008.04.011

81. S. J. Ryan, A. McNally, L. R. Johnson, E. A. Mordecai, T. Ben-Horin, K. Paaijmans, et al., Mapping physiological suitability limits for malaria in Africa under climate change, *Vector-Borne and Zoonotic Dis.*, **15** (2015), 718–725. https://doi.org/10.1089/vbz.2015.1822

82. J. Wu, R. Dhingra, M. Gambhir, J. V. Remais, Sensitivity analysis of infectious disease models: methods, advances and their application, *J. R. Soc. Interface*, **10** (2013), 20121018. https://doi.org/10.1098/rsif.2012.1018

83. R. G. McLeod, J. F. Brewster, A. B. Gumel, D. A. Slonowsky, Sensitivity and uncertainty analyses for a SARS model with time-varying inputs and outputs, *Math. Biosci. Eng.*, **3** (2006), 527. https://doi.org/10.3934/mbe.2006.3.527

84. J. Carboni, D. Gatelli, R. Lika, A. Saltelli, The role of sensitivity analysis in ecological modeling, *Ecol. Model.*, **203** (2006), 167–182. https://doi.org/10.1016/j.ecolmodel.2005.10.045

85. E. Iboi, A. Richardson, R. Ruffin, D. Ingram, J. Clark, J. Hawkins, et al., Impact of public health education program on the novel coronavirus outbreak in the United States, *Front. Public Health*, **9** (2021), 630974. https://doi.org/10.3389/fpubh.2021.630974

86. World Population Review, *Saudi Arabia Population 2021*, 2022. Available from: https://worldpopulationreview.com/countries/saudi-arabia-population.

87. The World Bank—Data, *Life Expectancy at Birth, Total (Years)–Saudi Arabia*, 2022. Available from: https://data.worldbank.org/indicator/SP.DYN.LE00.IN?locations=SA-AD

88. WLE, *Animal Life Expectancy*, 2021. Available from: https://data.worldbank.org/indicator/SP.DYN.LE00.IN?locations=SA-AD

89. S. Safdar, C. N. Ngonghala, A. Gumel, Mathematical assessment of the role of waning and boosting immunity against the BA. 1 Omicron variant in the United States, **20** (2023), 179–212. https://doi.org/10.3934/mbe.2023009

90. J. E. Park, S. Jung, A. Kim, MERS transmission and risk factors: a systematic review, *BMC Public Health*, **18** (2018), 1–15. https://doi.org/10.1186/s12889-018-5484-8

91. X. Jiang, S. Rayner, M. H. Luo, Does SARS-CoV-2 has a longer incubation period than SARS and MERS, *J. Med. Virol.*, **92** (2020), 476–478. https://doi.org/10.1002/jmv.25708

92. Centers for Disease Control and Prevention (CDC), MERS coronavirus in dromedary camel herd, Saudi Arabia, *Emerging Infect. Dis.*, **20** (2022), 1231–1234. https://doi.org/10.3201/eid2007.140571

93. C. N. Ngonghala, H. B. Taboe, S. Safdar, A. B. Gumel, Unraveling the dynamics of the Omicron and Delta variants of the 2019 coronavirus in the presence of vaccination, mask usage, and antiviral treatment, *Appl. Math. Modell.*, **114** (2023), 447–465. https://doi.org/10.1016/j.apm.2022.09.017

94. A. B. Gumel, E. A. Iboi, C. N. Ngonghala, G. A. Ngwa, Toward achieving a vaccine-derived herd immunity threshold for COVID-19 in the US, *Front. Public Health*, **9** (2021), 709369. https://doi.org/10.3389/fpubh.2021.709369

95. A. B. Gumel, E. A. Iboi, C. N. Ngonghala, G. A. Ngwa, Mathematical assessment of the roles of vaccination and non-pharmaceutical interventions on COVID-19 dynamics: a multigroup modeling approach, **2020** (2020).

96. M. G. Hemida, A. Elmoslemany, F. Al-Hizab, A. Alnaeem, F. Almathen, B. Faye, et al., Dromedary camels and the transmission of middle east respiratory syndrome coronavirus (MERS-CoV), *Transboundary Emerging Dis.*, **64** (2017), 344–353. https://doi.org/10.1111/tbed.12401

97. S. E. Eikenberry, M. Mancuso, E. Iboi, T. Phan, K. Eikenberry, Y. Kuang, et al., To mask or not to mask: Modeling the potential for face mask use by the general public to curtail the COVID-19 pandemic, *Infect. Dis. modell.*, **5** (2020), 293–308. https://doi.org/10.1016/j.idm.2020.04.001

Appendix A: Initial conditions used in numerical simulations

(1) Initial conditions for Figure 8:
$(S_H(0), V_H(0), E_H(0), I_{HA}(0), I_{HS}(0), I_{HH}(0), R_H(0), S_C(0), V_C(0), I_C(0), R_C(0),)$ = (9,900,000, 0, 10, 100, 100, 10, 1, 3,900,000, 0, 10, 977, 1).

(2) Initial conditions for Figure 10:
$(S_H(0), V_H(0), E_H(0), I_{HA}(0), I_{HS}(0), I_{HH}(0), R_H(0), S_C(0), V_C(0), I_C(0), R_C(0),)$ = (36,617,538, 0, 1, 1, 1, 1, 1, 1,400,000, 0, 1, 7, 1).

(3) Initial conditions for Figure 12:
$(S_H(0), V_H(0), E_H(0), I_{HA}(0), I_{HS}(0), I_{HH}(0), R_H(0), S_C(0), V_C(0), I_C(0), R_C(0),)$ = (36,617,538, 0, 2196, 1, 1, 1, 1, 1,400,000, 0, 60, 977, 0).

(4) Initial conditions for Figure 13:
$(S_H(0), V_H(0), E_H(0), I_{HA}(0), I_{HS}(0), I_{HH}(0), R_H(0), S_C(0), V_C(0), I_C(0), R_C(0),)$ = (36,617,538, 0, 1, 1, 1, 1, 1, 1,400,000, 0, 1, 7, 1).

(5) Initial conditions for Figure 14:
$(S_H(0), V_H(0), E_H(0), I_{HA}(0), I_{HS}(0), I_{HH}(0), R_H(0), S_C(0), V_C(0), I_C(0), R_C(0),)$ = (36,617,538, 0, 2196, 1, 1, 1, 1, 1,400,000, 0, 60, 977, 0).

(6) Initial conditions for Figure 15:
$(S_H(0), V_H(0), E_H(0), I_{HA}(0), I_{HS}(0), I_{HH}(0), R_H(0), S_C(0), V_C(0), I_C(0), R_C(0),)$ = (9,000,000, 10, 10, 100, 100, 100, 1, 50,000, 100, 10, 9700, 1).